STUDY OF SPRING BACK EFFECT AND IMPROVEMENT OF THE GEOMETRIC ACCURACY IN SPIF PROCESS

By

ABHISHEK J. SUTHAR

(16MMCC25)

DEPARTMENT OF MECHANICAL ENGINEERING
INSTITUTE OF TECHNOLOGY
NIRMA UNIVERSITY
AHMEDABAD-382481

MAY 2018

STUDY OF SPRING BACK EFFECT AND IMPROVEMENT OF THE GEOMETRIC ACCURACY IN SPIF PROCESS

Major Project Report

Submitted in partial fulfillment of the requirements

For the Degree of

Master of Technology in Mechanical Engineering

(CAD-CAM)

By

ABHISHEK J. SUTHAR

(16MMCC25)

Guided By

Prof. A. M. Gohil

Dr. B. A. Modi

DEPARTMENT OF MECHANICAL ENGINEERING
INSTITUTE OF TECHNOLOGY
NIRMA UNIVERSITY
AHMEDABAD-382481
MAY 2018

Declaration

This is to certify that

- The thesis comprises of my original work towards the degree of Master of Technology in Mechanical Engineering (CAD-CAM) at Nirma University and has not been submitted elsewhere for a degree.
- Due acknowledgment has been made in the text to all other material used.

ABHISHEK J. SUTHAR

16MMCC25

Undertaking for Originality of the Work

I, **Abhishek J. Suthar**, Roll. No. **16MMCC**25, gives undertaking that the Major Project Report entitled "**Study of Spring back effect and improvement of the geometric accuracy in SPIF process**" submitted by me, towards the partial fulfillment of the requirements for the degree of Master of Technology in Mechanical Engineering (CAD-CAM) of Nirma University, Ahmedabad, is the original work carried out by me and I give assurance that no attempt of plagiarism has been made. I understand that in the event of any similarity found subsequently with any published work or any dissertation work elsewhere; it will result in severe disciplinary action.

Signature of Student

Endorsed by

(Signature of Guide)

Date:

Place: Ahmedabad

Certificate

This is to certify that the Major Project Report entitled "**Study of Spring back effect and improvement of the geometric accuracy in SPIF process**" submitted by **Mr. Abhishek J. Suthar (16MMCC25)**, towards the partial fulfillment of the requirements for the award of the Degree of Master of Technology in Mechanical Engineering (CAD-CAM) of Institute of Technology, Nirma University, Ahmedabad is the record of work carried out by him under our supervision and guidance. In our opinion, the submitted work has reached a level required for been accepted for examination. The result embodied in this major project, to the best of our knowledge, has not been submitted to any other University or Institution for award of any degree.

Dr. B. A. Modi
Co-Guide and Professor,
Department of Mechanical Engineering,
Institute of Technology,
Nirma University,
Ahmedabad.

Prof. A. M. Gohil
Guide and Assistant Professor,
Department of Mechanical Engineering,
Institute of Technology,
Nirma University,
Ahmedabad.

Dr. V. J. Lakhera
Professor and Head,
Department of Mechanical Engineering,
Institute of Technology,
Nirma University,
Ahmedabad

Dr. Alka Mahajan
Director,
Institute of Technology,
Nirma University,
Ahmedabad

Acknowledgements

I want to show my gratitude to those who have helped me throughout my project work and presentations. First of all, I would like to thank my internal project Guide Prof. A. M. Gohil for providing valuable guidance. I am grateful for patience and interest he has shown towards me.

Then I express my sincere gratitude towards the project co-guide Dr. B. A. Modi who always stretch my limitations and made me capable enough to work on the project.

I would like to thank Dr. V. J. Lakhera (HOD, Mechanical engineering department, Institute of Technology, Nirma University), Dr. Alka Mahajan (Director, Institute of Technology, Nirma University) for providing me required facility to carry out project work.

I would like to thank whole mechanical workshop department(Institute of Technology, Nirma University) for their required support throughout project work.

The blessings of God and support of my parents encouraged me which led to a successful project work for which I am very much grateful to them.

I am also thankful to all my dear friends for their motivation and every possible help.

-Abhishek J. Suthar

16MMCC25

Abstract

Single Point Incremental Sheet Forming (SPIF) process is a recent development in sheet metal forming industry. The process has advantage of high formability, flexibility and low tooling cost. However, the process is suffering the drawback of poor accuracy. In the present work, effect of tool diameter and step depth on geometric accuracy and pillow defect have been studied. For the experimental work AA1100-F aluminum sheet is used. Annealing process has been performed on each blank before carrying out experiential work. By using electronic edge finder geometric accuracy and pillow defect have been measured in clamped position on VMC machine. FEA analysis is also performed using LS-DYNA Software.

Contents

List of Figures

List of Tables

Abbreviation

ISF	Incremental sheet forming
SPIF	Single point incremental forming
TPIF	Two point incremental forming
FLD	Forming limit diagram
DOE	Design of experiment
CNC	Computer Numerical control
r	Radius
sd	Step Depth

Chapter 1

Introduction

Incremental shaping is an imperative method in which framing of sheet metal is finished by a hemispherical framing apparatus. It is a system for a sheet metal which is distorted by cutting edge and confined plastic disfigurement utilizing a general hemispherical instrument and it is performed on a VMC machine. This procedure is regularly utilized for assembling of items in unimportant bunches. In the traditional shaping procedure, kick the bucket and punch are noteworthy elements. Change fit as a fiddle or size of any coveted item changes the character and size of pass on and punch. Tooling cost is high in the preservationist procedure, ISF the tooling cost is low as a solitary apparatus is utilized. While in ISF process sheet is clipped by a clear holder and hemispherical instrument is moved utilizing CNC machine. The fundamental segments of ISF process are as appeared in the Schematic outline (Fig 1.1).

1) VMC machine,
2) Hemispherical tool,
3) Clamping and backing plate

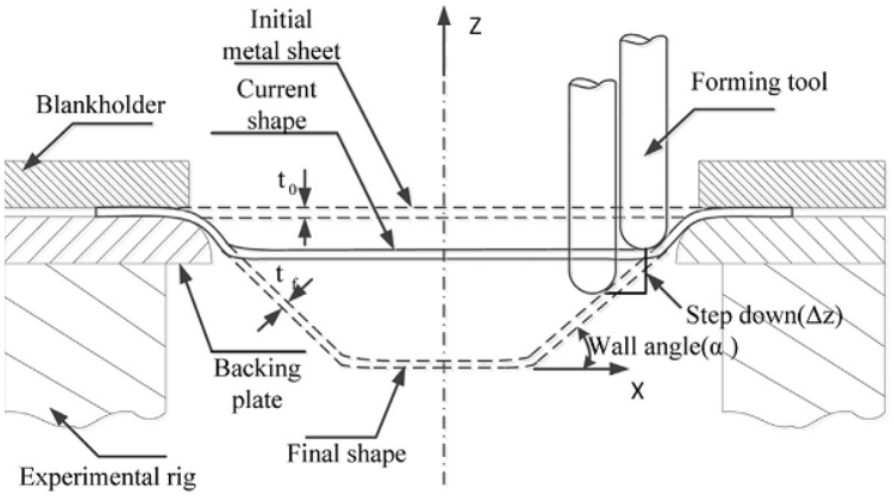

[1]

Figure 1.1: Schematic Representation of SPIF Process

1.1 Spring back effect

Springback is the geometry change made to a section toward the finish of the shaping procedure when the part has been discharged from the powers of the framing apparatus. Endless supply of sheet metal framing, profound drawn and extend stepped parts spring back and there by influence the dimensional exactness of a completed part. The last type of part is changed by springback, which makes it hard to deliver the part.

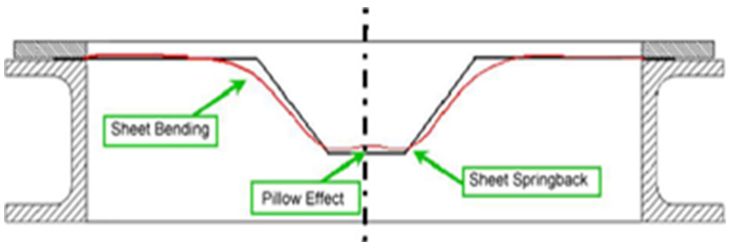

[2]

Figure 1.2: Spring back effect

1.2 Advantages of Incremental Sheet Forming

Advantages of ISF process which are as follows-

1. In this procedure, There is no prerequisite of either positive or negative kick the bucket amid the procedure
2. It is an exceedingly adaptable process.
3. On account of progress of complex part in the plan, it is required to change the apparatus way.
4. The ease of Rapid Prototyping of metal sheet segment with the procedure.
5. The span of the part relies upon the measure of the machine.
6. The operation is inconspicuous and relatively blast (clamor) free.

1.3 Disadvantages of Incremental Sheet Forming

Disadvantages of ISF which are as follows-

1. It is limited for the small size production.
2. During the process, spring back effect is very high.
3. Required forming time of the process is greater than another process.

.

1.4 Application

There are some imperative utilizations of ISF which are as per the following The ISF procedure is exceptionally relevant according to the coveted segment like in avionic business where the instrument board, body board, traveler situate cover, and so forth effortlessly produced by it with constrained time. Aside from avionic business, the ISF procedure has extraordinary necessity like entryway inward/external board, hood board, motor cover, and so forth effectively made with the coveted shape. It is exceptionally appropriate in tweaked items like denture plate, lower leg bolster, metal head protector, and so on effortlessly worked with required shape and size. Aside from these, the ISF procedure is likewise profoundly pertinent to mobile phones, IC lead outlines, gadgets items, social insurance, small scale latches, results of national security and barriers, and so forth.

1.5 Objectives

Following are the objectives of the project work:

1. To study the effect of process parameters on geometric accuracy in SPIF process

2. To study the effect of process parameters on spring back in SPIF process

1.6 Methodology

Following methodology is adopted

1. Annealing Process
2. Material Characterization
3. Preparation of blank
4. Design of experiments using Minitab
5. Experimental work on SPIF using Vertical Machining Center (VMC) Measurement of Geometric Accuracy
6. Experimental work on SPIF using Vertical Machining Center (VMC) Measurement of Spring back
7. FE Analysis using LS-DYNA software

Chapter 2

Literature Review

2.1 Review of research papers related to single point incremental forming process

L-W Ma and J-H MGabriel Centeno , Isabel Bagudanch, A. J. Martinez-Donaire, M. L. Gracia-Romeu, C.Valleano [3], Failure in SPIF experiment analysis of the independent determination of conventional formability limits by necking and fracture performing various test, optical deformation measurement system with digital image correlation technique was used for strain distributions at outer surface of the tested sheet. The author concluded that that the enhancement of formability above the Forming Limit Curve (FLC) in SPIF is much higher than in stretch-bending .

G. Hussain, L. Gao[4],The diminishing furthest reaches of the sheet metal in SPIF is checked by the Cosine's law tf = t0*cos for thickness circulation. The technique for Lowest conceivable of diminishing sheet which is decrease handling time and cost.

K. A. Al-Ghamdi , G. Hussain & Shahid I. Butt [5],This paper speaks to the utilization to all the while anticipate and upgrade the power and in addition abandons assessment in SPIF process. Influence the shaping power in SPIF the power increments with increment in the measure of divider , the power diminishes with the expansion in the corner-overlay estimate. The development of imperfections, the parameters indicate exceedingly associated impacts are hard to foresee with sensible exactness utilizing the explanatory recipes on the powers .

Singh, Arshpreet, and Anupam Agrawal [6], Impact of anisotropy in the disfiguring powers and spring back is incorporated into twisting examinations. Ductile testing was finished by ASTM-E8 norms for sheet metals. The powers initiated in incremental bowing are right around 33% lower than regular bowing. The spiral blunder for disfigurement machining (DM) extending mode segments is lower than incremental extend framed sheet metal parts .

G. Hussain , H. R. Khan , L. Gao & N. Hayat [7], This paper gives brief thought regarding the rules for apparatus estimate choice in SPIF process. High thickness and most minimal conceivable apparatus estimate can't enhanced Spifability . DOE is utilized for getting ready exploratory work and FE examination utilizing LS-DYNA.

A. Petek , K. Kuzman , B. Suhac [8], The creator suggested that utilizing the shaping power time arrangement in the analytic framework permits quick and solid crack recognition and confinement. The framing power reacts well to little varieties showing up amid the shaping procedure.

Kurra Suresh , Srinivasa Prakash Regalla [9],Numerical reenactment discover the formability of profound illustration sheet. Formability of changing funnel shaped divider point and pyramidal frustums with round, circular, illustrative and exponential creates which are dissected in LS-DYNA utilizing systematic framing limit bend.

J. Leóna, D. Salcedo, C. Ciáurriza, C.J. Luis, J.P. Fuertes, I. Puertas, R. Luri [10], In this examination work, the impact of various outline factors that are engaged with the SPIF procedure have been considered by limited components reproductions and utilizing the DOE system so as to design and to enhance the investigation. The creator reasoned that misshapening and the turns of the winding increments when the punch range is diminished, the punch compel achieves a lower esteem.

L. Fratini , G. Ambrogio , R. Di Lorenzo , L. Filice, F. Micari [11], The real resist crack in plane strain condition was resolved for various materials and principle material parameters like strain solidifying coefficient , ordinary anisotropy , extreme elasticity and rate stretching. At different of clear material which impact of every property on material formability . A powerful reaction surface was setup in SPIF strain solidifying coefficient, level of lengthening most elevated and formability is biggest.

E Hagan and J Jeswiet [12], A Non-contact strategy utilizing white light interferometry was chosen to abstain from scratching the material surface. Looked at the hypothetical and measured profile statures. surfaces framed with different profundity increases demonstrate an exponential increment in the most extreme top to tallness as the addition measure diminished.

Joost Duflou , Yasemin Tunc¸kol , Alex Szekeres, Paul Vanherck [13],In this paper the part disappointment expectation in light of state of power bend is clarified for the tried materials, systematic outcomes and the initiated powers are displayed and constrain bend can be utilized as disappointment forecast pointer. Power measured by a table sort dynamometer and its concentrated on an alternate parameters like, 1) Instrument distance across 2) Step profundity 3) Thickness of sheet 4) vertical advance size.

W.C. Emmensa , A.H. van den Boogaard [14], The creators directs the fluctuates test like Effects of shear, contact shear, bowing hydrostatic weight. They talked about the limited distortion Local diminishment of the elastic yield compel just balances out the twisting and furthermore the confined misshapening is because of the geometric impact, and nearby decrease of the pliable yield drive .

Ghulam Hussain [15], The author conduct the experimental work and they compare with the Finite element analysis of Incremental sheet metal forming simulation is carried out by using LS-DYNA.

I. Bagudancha , M.L. Garcia-Romeua, I. Ferrera, J. Lupiañez [16], The author conduct the experimental work and they compare with the Finite element analysis of Incremental sheet metal forming simulation is carried out by using LS-DYNA.

Mehdi Vahdati, Ramezanali Mahdavinejad and Saeid Amini [17],This article exhibits the procedure of outline, examination, produce and testing of a vibrating shaping instrument for the improvement of ultrasonic vibration– helped incremental sheet metal framing. In this article, the procedure of plan ,investigation, manufacture And testing of a vibrating shaping device for advancement of UVaISMF was exhibited.

Carlos Felipe Guzmán , Jun Gu , Joost Duflou , Hans Vanhove , Paulo Flores , Anne Marie Habraken [18],In this article, a two-slope SPIF pyramid with two distinct profundities, which experiences vast geometric deviations when contrasting the expected and last shapes, is examined. Keeping in mind the end goal to approve the model, the state of a transversal cut and the pivotal drive advancement amid the procedure were looked at. **Julian M. Allwood , Daniel**

Braun , Omer Music [19], This paper proposes and looks at another approach in which the zone to be framed inside the clear is "somewhat removed" utilizing a water stream or laser cutter. it appears that the utilization of mostly cut-out spaces does not give a valuable advantage in incremental sheet shaping.

KA Al-Ghamdi and G Hussain [20],The cushion is an imperfection that unfavorably influences the geometrical precision and also the formability in single-point incremental framing. This investigation with an essential target to overcome padding in SPIF by controlling the properties of material.

Bagudanch , M.L. Garcia-Romeua , G. Centeno , A. Elías-Zú˜niga , J. Ciurana [21], The gadget impact of the shaft does not just have the capacity of diminishing the most extreme framing power, yet additionally expands the sheet formability which is assessed by the greatest profundity accomplished and impacts surface unpleasantness. Which can be Increment of temperature got because of the rubbing between the device and the sheet clear, and material properties of thermoplastic polymers are influencing .

L-W Ma and J-H Mo [22],In this paper, block components are utilized to build up the entire threedimensional FEM demonstrate and a streamlined three- dimensional FEM model of a truncated cone and truncated pyramid. From the reenactment result, the nitty gritty data, for example, powerful strain dispersion was given and it is useful to comprehend the framing standard of SPIF. **Crina Radu and**

Catalin Tampu [23], It was discovered that an ideal condition of leftover burdens and certainly a decent precision of parts can be acquired when little estimations of hardware measurement and device vertical advances, separately high estimations of bolster rate and shaft speed are utilized.

D Young and J Jeswiet [24], Twofold pass framing can permit the creation of parts that thin to disappointment with single-pass systems.

Chapter 3

Preliminary Experiment

To meet the objectives of the present work the methodology as described in Chapter 1 has been followed.

3.1 Annealing

Strengthening is a general term used to portray the rebuilding of a frosty worked or warmth treated metal or compound to its unique properties, in order to build pliability (and subsequently formability), lessen hardness and quality, or adjust the smaller scale structure. Toughening is additionally to ease leftover worries in a produced part for enhanced machinability and measurement steadiness. The term toughening likewise applies to warm treatment of glasses and comparable items and weldments

The strengthening procedure includes (1) warming the work piece to inside a particular scope of temperatures, (2) holding it at that temperature for a timeframe, and (3) cooling it gradually. The procedure might be done in a dormant or controlled climate or performed at low temperatures to avert of limit surface oxidation, Annealing temperatures might be higher than the re-crystallization temperature, contingent upon the level of icy work (and thus put away vitality).

Annealing Process is performed in Muffle Furnace. Three Sheets of Aluminum grade AA1100-F have been heated to a temp of 343℃ with a holding time of 10, 20 & 30 min. Furnace cooling is used after heating and holding the sheet at 343 ℃.

To grip the sheet metal specimen for the measurement of grain size cold mounting technique has been used which is shown in Fig 3.1 & 3.2.

Figure 3.1: Before Cold Mounting

Figure 3.2: After Cold Mounting

Polishing process has been done after cold mounting process. During the polishing process different size of mesh paper have been used for rough polishing. Finish polishing is done using diamond paste of 1 and 3 micron size.

After polishing process, etchant is applied on the specimen surface to reveal grain boundaries. Chemicals used to make the etchant are given in Table 3.1.

Table 3.1: Chemical composition of Etchant

Etchant	Conc.	Condition	Metal
Methanol	25 ml	10 - 60 seconds	Pure Aluminum
Hydrochloric acid	25 ml		
Nitric acid	25 ml		
Hydrofluric acid	1 drop		

Measurement of Grain Size

After etching, grain size has been determined at 500X magnification level using image analyzer. The result of measurement is given in Fig. 3.3 for the sheet which was kept at 343 ℃ for 10 min heating time.

This figure shows the grain size for 10 min experiment of after annealing.

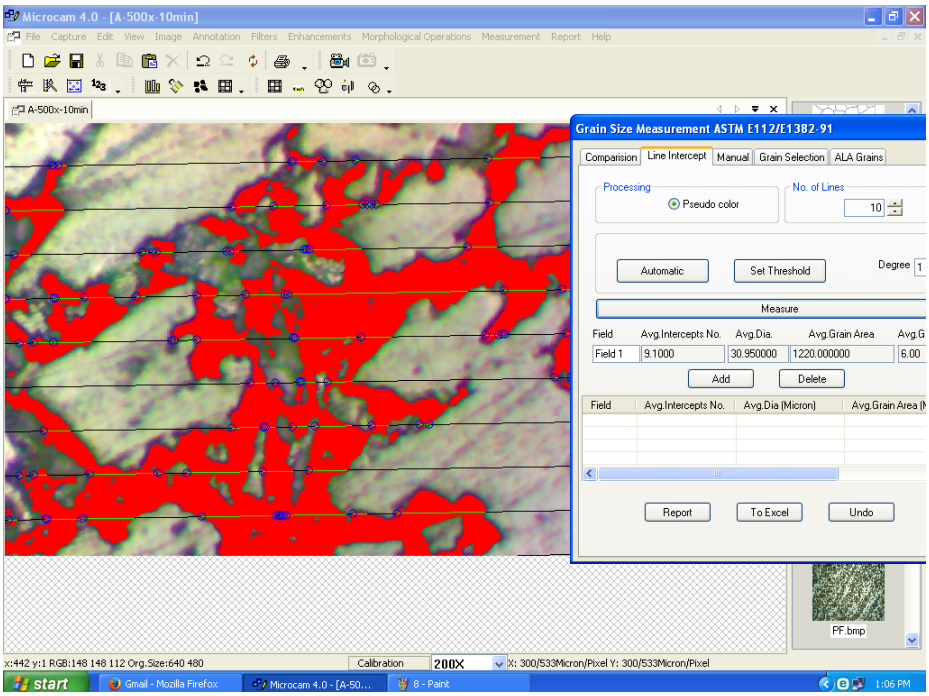

Figure 3.3: Grain size measurement using line intercept method

Grain Size has been determined as per ASTM E112/E1382-91 using line intercept method. After annealing grain size is found to be 6 micron as against 5 micron before annealing.In the same way grain size measurement have been carried out and the results are summarized in Table 3.2.

Table 3.2: Grain Size Measurement

Grain Size		
Time (min)	Before Annealing at 500x (micron)	After Annealing at 500x (micron)
10	5	6
20	4	6
30	7	7

Measurement of Hardness

Micro hardness measurement has been carried out by using Micro Vicker hardness tester. Fig 3.4 and Fig 3.5 shows indentation on the sheet metal surface during before and after annealing condition respectively. Table 3.3 gives the summary of hardness obtained before and after annealing process.

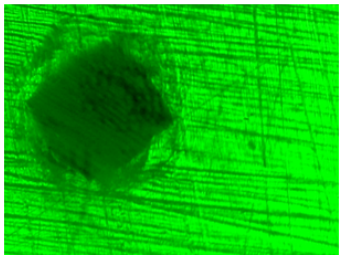

Figure 3.4: Indentation Before Annealing

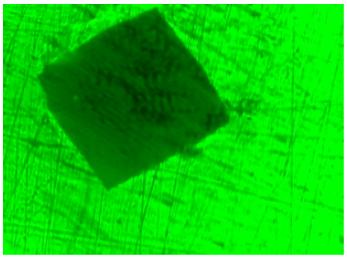

Figure 3.5: Indentation After Annealing

Table 3.3: Hardness of the Aluminum sheet

HARDNESS (HVN)											
			Before Annealing				After Annealing				
Exp. No.	Temp	Time	1	2	3	Average	1	2	3	Average	Reduce
	(℃)	(min)									(%)
1	343	10	30.2	31.7	30.9	30.9	21.2	23.5	26.3	23.66	23.43
2	343	20	28.3	30.3	27.1	28.5	21.3	24.5	23.7	23.16	18.73
3	343	30	44.4	48.8	50.8	48	28	28.4	29.4	28.6	40.62

From the hardness measurement data it can be seen that after annealing, hardness of the specimen reduces by 18.73 to 40.62 %.

Based on the experiment, as 6 micron grain size is appropriate for the sheet metal industry, for all experiment annealing process is carried out at 343 ℃ and holding time of 10 min.

3.2 Geometry of Component

It is proposed to study the effect of process parameters on geometric accuracy of aluminum sheet. Component shape selected is cone with straight line as generatix as shown in Fig 3.6.

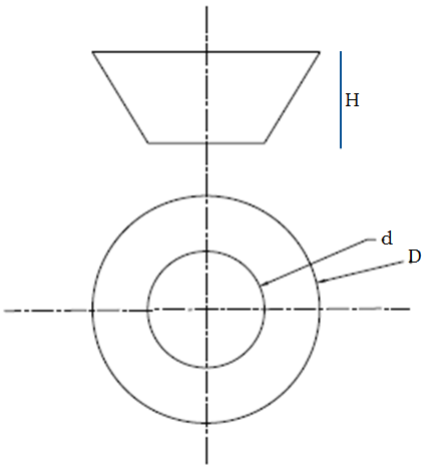

Figure 3.6: Cone Geometry

3.3 Experiment setup for SPIF

Experiments are carried out on VMC machine-Jyoti CNC PX-10 having the Siemens controller. It is a 3-Axis machine with positioning accuracy of 0.01mm and repeatability of 0.005 mm. In this work, Single Point Incremental Forming process is used to investigate the formability of aluminum sheet performing the cone test. Experimental setup used for the work is shown in Fig. 3.7.

Figure 3.7: Experimental setup

Fixture is made from EN31 material. Clamping plate and backing plate are of 200 mm * 200 mm * 12 mm of size. Backing plate and Clamping plate are having a 80 mm and 90 mm circular cut out respectively as shown in Fig. 3.8.

[25]

Figure 3.8: Fixture For Experimental work

3.4 Material Characterization

The materials used for the experimental work has been (Aluminum alloy - AA1100 of 1mm thickness) characterized using the tensile test prescribed by ASTM A370/ASTM E8 standard. After annealing process, Tensile testing has been carried out. Based on the load extension diagram provided by the testing laboratory, true stress-true strain curve have been obtained. The test results are summarized in Table. 3.4.

Table 3.4: Material Characterization

Sr. No.	Material property	1 mm thick sheet
1	Yield stress (N/mm2)	44.523
2	UTS (N/mm2)	72.642
3	Elongation (%) in 50mm gauge length	18.44
4	Strain hardening exponent (n)	0.4715
5	Strength co-efficient (K)	197.1064
6	Young modulus (MPa)	56843
7	Poisson's ratio	0.33

3.5 Design of Experiments

Following factors have been considered for experimental work which is based on literature study:

(1) Tool Radius

(2) Step Depth

For the experiment tool size is selected at 3 different levels 4, 5 & 6 mm and step depth at 3 different levels of 0.25, 0.5 and 0.75 mm.

D.O.E. has been carried out using minitab software as shown in Table 3.5.

Table 3.5: Design of Experiment

StdOrder	RunOrder	PtType	Blocks	Tool Radius	Step Depth
7	1	1	1	6	0.25
5	2	1	1	5	0.5
1	3	1	1	4	0.25
6	4	1	1	5	0.75
4	5	1	1	5	0.25
3	6	1	1	4	0.75
2	7	1	1	4	0.5
8	8	1	1	6	0.5
9	9	1	1	6	0.75

Some of the factors which are kept constant during the process are as shown in Table 3.6 .

Table 3.6: Constant Parameters

Sr. No.	Parameters	Value
1	Shape	Cone
2	Feed(mm/min)	500
3	Program Strategy	Constant Z-depth
4	Tool Rotation	No tool rotation
5	Material Type	Aluminum AA1100-F
6	Lubricant oil	Mineral Oil

Geometric accuracy and size of the pillow defect have been considered as a response variable and they are measured using electronic edge finder.

3.6 Blank Preparation

For the study of formability, Blank is prepared for strain measurement as per ASTM E 2218-02 standard, the grid pattern geometry as shown in Fig 3.9.

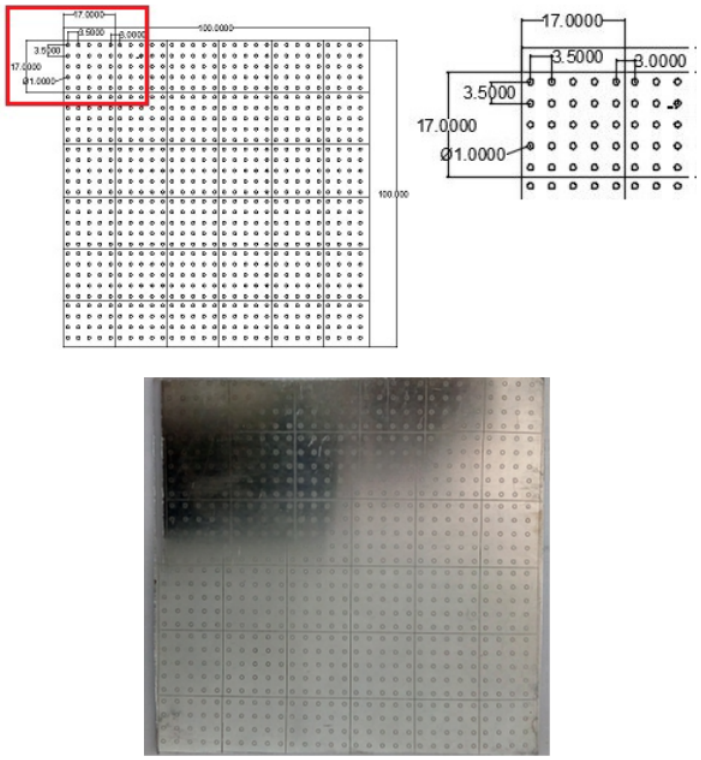

Figure 3.9: Engraved Sheet

3.7 Results And Discussion

Measurement has been measured as geometry drawing, it shown in fig 3.12. Reading has been taken at various height and different location of bottom of the cone.

As per the geometry described in Fig 3.1, components have been formed. All the formed components are presented in the Fig 3.10.

Figure 3.10: Deformed sheet

Experimental height of formed component is measured using electronic edge finder as show in Fig 3.11. To accurately compare theoretical and experimental values tool length and edge finder length have been taken from the same reference point. After performing the experiment edge finder is moved to touch the lowest point at X=0 and Y=0 to obtain experimental height. Number of such readings have been taken at equal interval of 5 mm along X axis and Y axis as shown in Fig. 3.12. The results for all the run order are summarized in Table 3.7.

Figure 3.11: Electronic Edge Finder

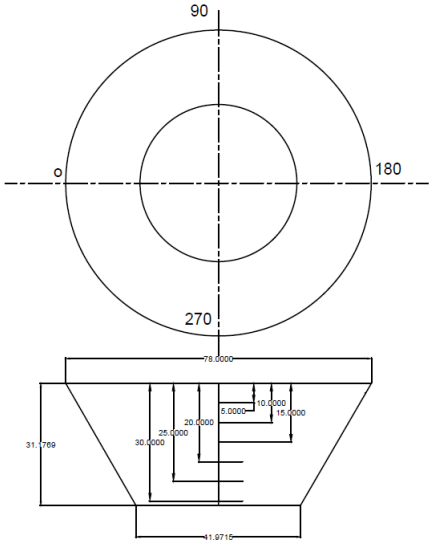

Figure 3.12: Geometry for Pillow Reading

Table 3.7: Pillow Defect

Exp. No.	Run Order	Original Height (mm)	Actual Height (mm)	Pillow Effect (mm)
1	1	31.1769	30.847	0.3299
2	2	31.1769	31.144	0.0329
3	3	31.1769	30.717	0.4599
4	4	31.1769	31.086	0.0909
5	5	31.1769	30.816	0.3608
6	6	31.1769	30.364	0.8129
7	7	31.1769	30.637	0.5399
8	8	31.1769	30.895	0.2819
9	9	31.1769	30.785	0.3919

The difference between the original and the actual height is considered as a pillow defect (H-h) which is shown in Table 3.7. Fig 3.13 to Fig 3.21 gives the diagram for pillow defect measurement taken at regular intervals of 5 mm along X and Y axis.

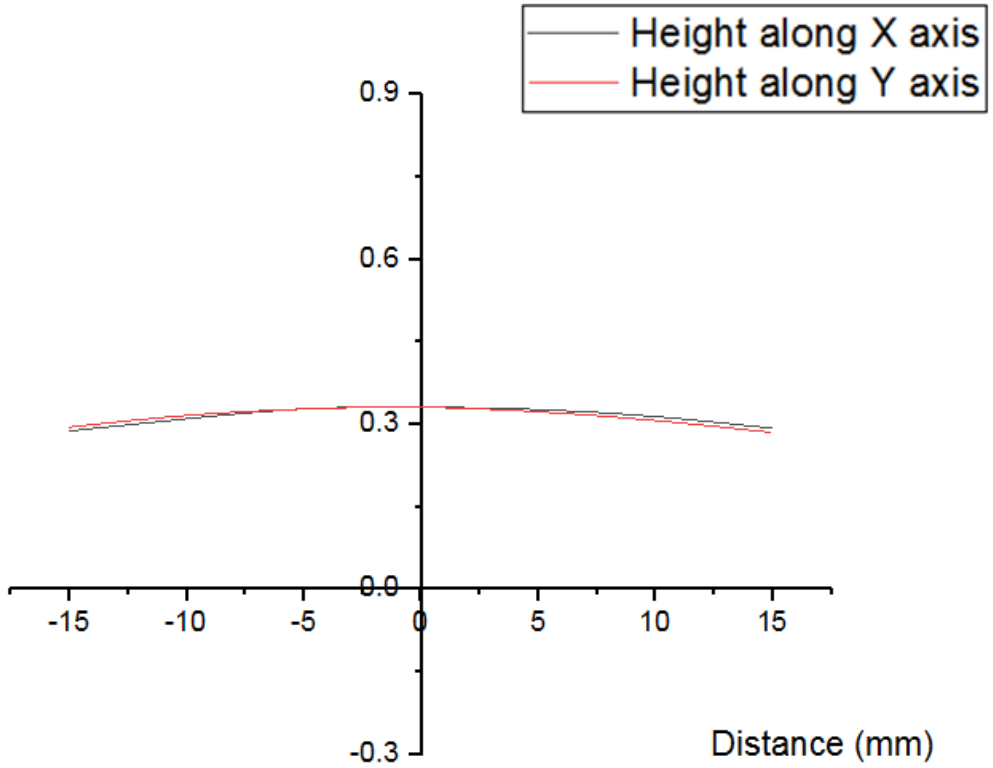

Figure 3.13: Pillow Defect Diagram for X and Y axis of RO1

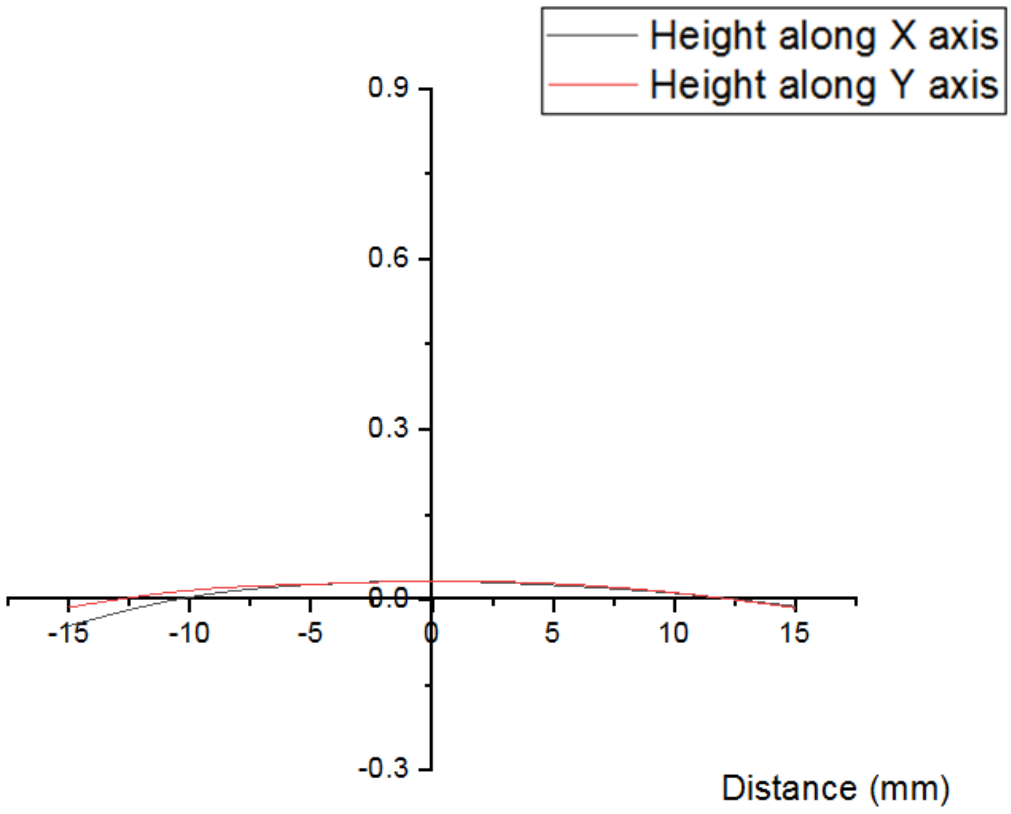

Figure 3.14: Pillow Defect Diagram for X and Y axis of RO2

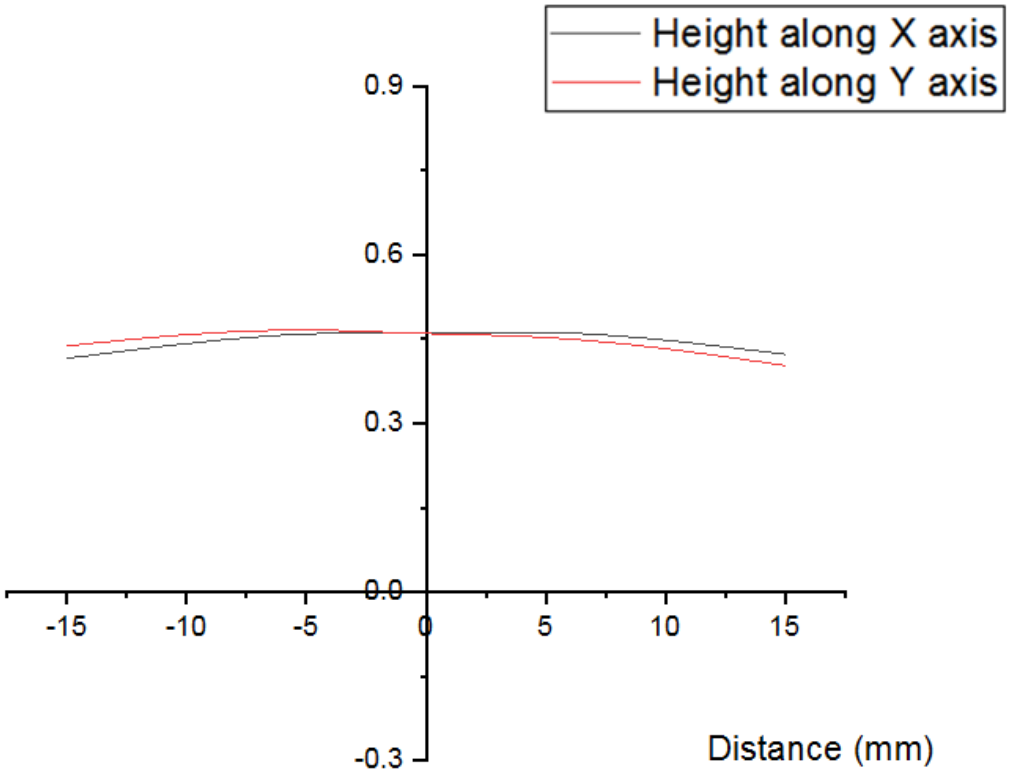

Figure 3.15: Pillow Defect Diagram for X and Y axis of RO3

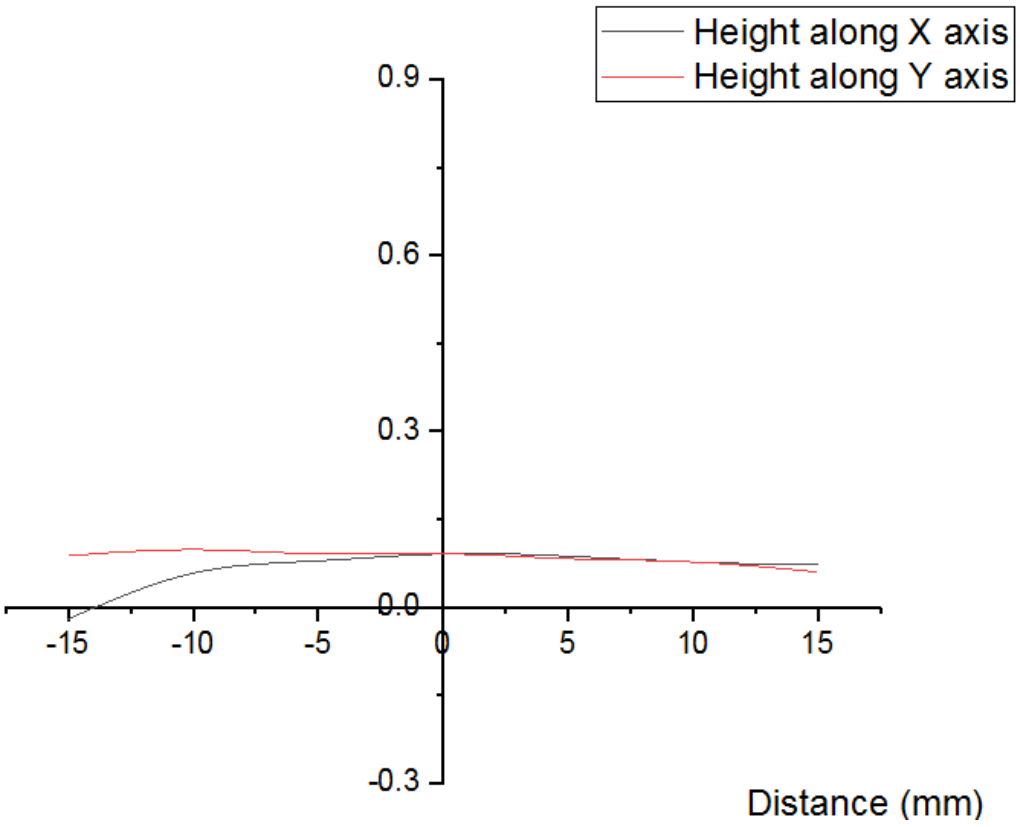

Figure 3.16: Pillow Defect Diagram for X and Y axis of RO4

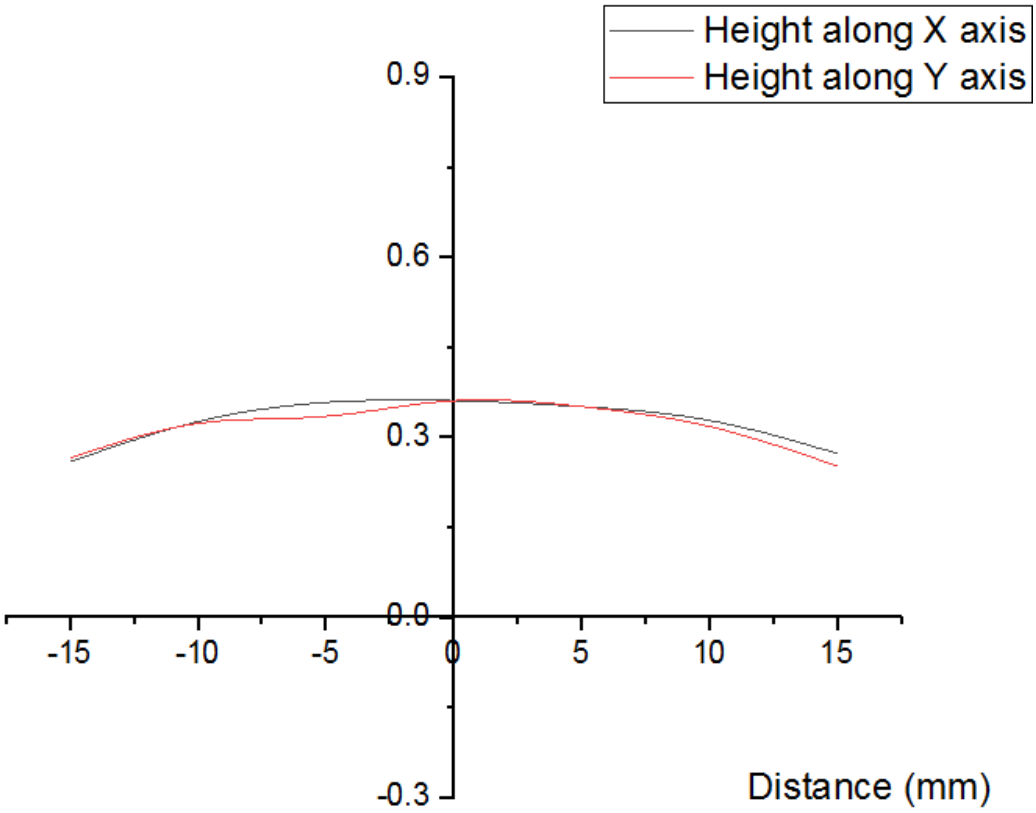

Figure 3.17: Pillow Defect Diagram for X and Y axis of RO5

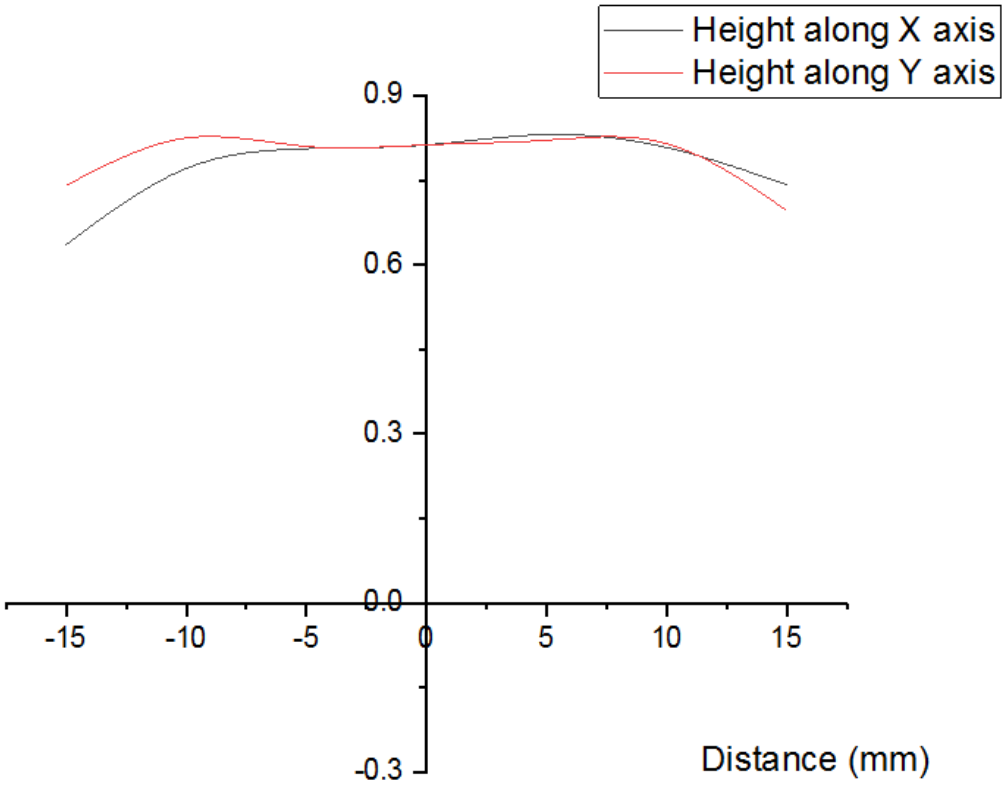

Figure 3.18: Pillow Defect Diagram for X and Y axis of RO6

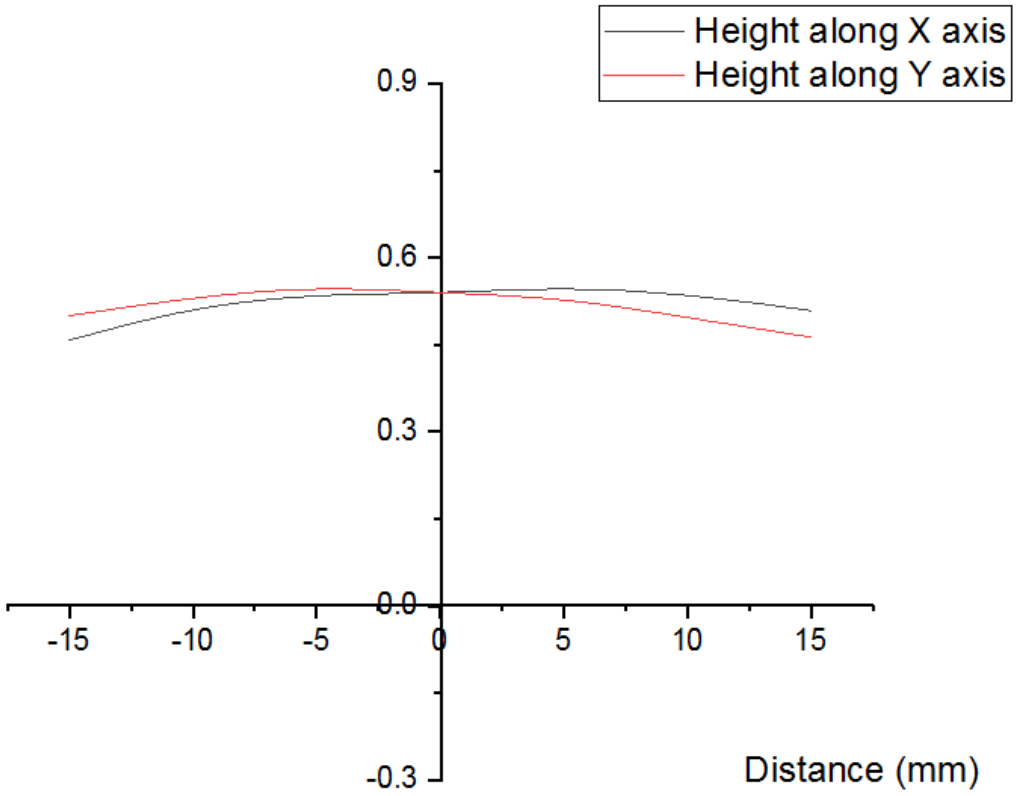

Figure 3.19: Pillow Defect Diagram for X and Y axis of RO7

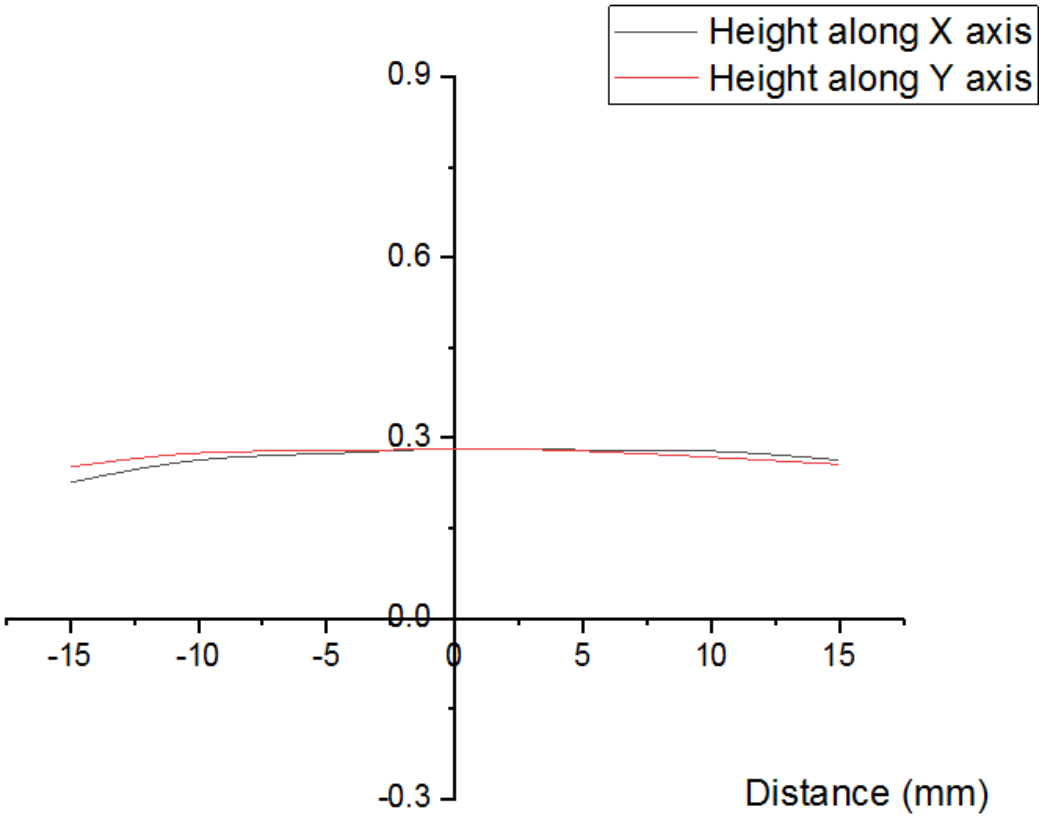

Figure 3.20: Pillow Defect Diagram for X & Y axis of RO8

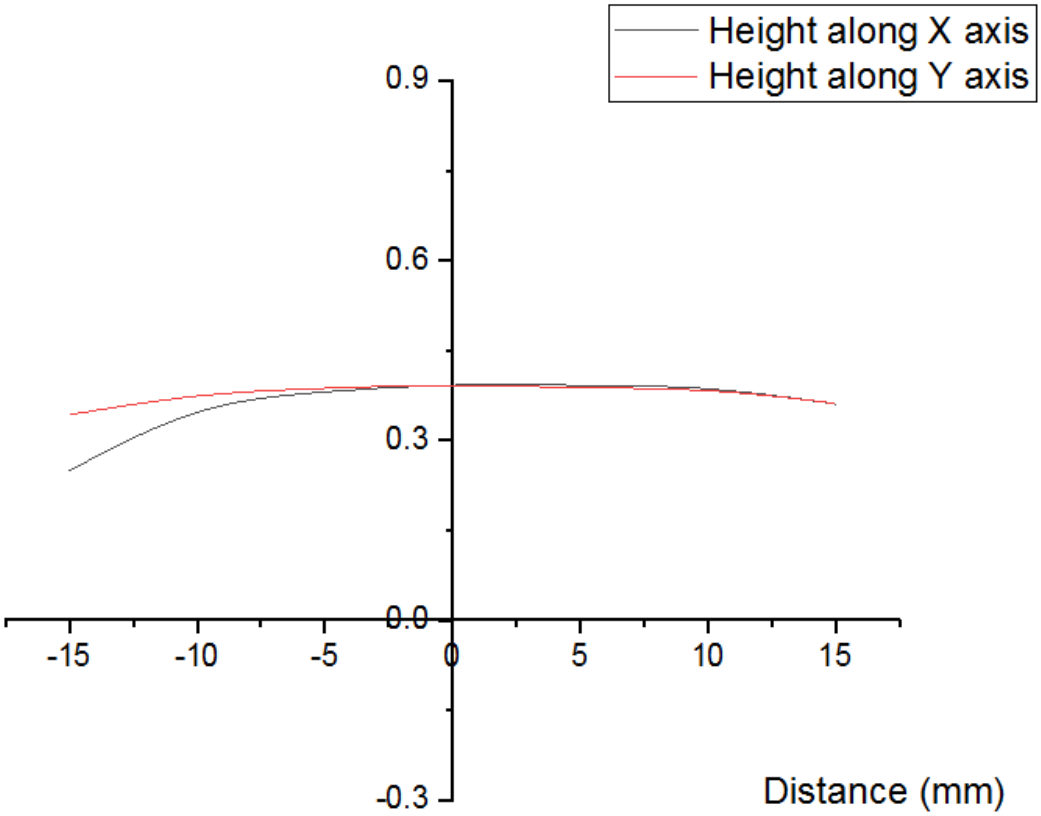

Figure 3.21: Pillow Defect Diagram for X & Y axis of RO9

3.8 Geometry Accuracy

For the measurement of geometry accuracy edge finder is moved to the different depth starting from 5 mm to 30 mm. At this constant depths edge finder is moved along positive 0°,90°,180° and 270° positions till it touches the work piece. When the edge finder touches the work piece X,Y and Z positions are noted down. The position obtained is of the bottom most tool reference point, however, the edge finder makes contact at other point. Hence based on this position spline is created tangent to all the circles representing the tool radius to obtain the actual profile of the work piece as shown in Fig 3.23. Geometric error is measured as maximum difference between actual and theoretical profile. Table 3.8 gives the summary of maximum geometric deviation obtained in different Run order. Table 3.8 to Table 3.19 gives the position data obtained for the different Run order.

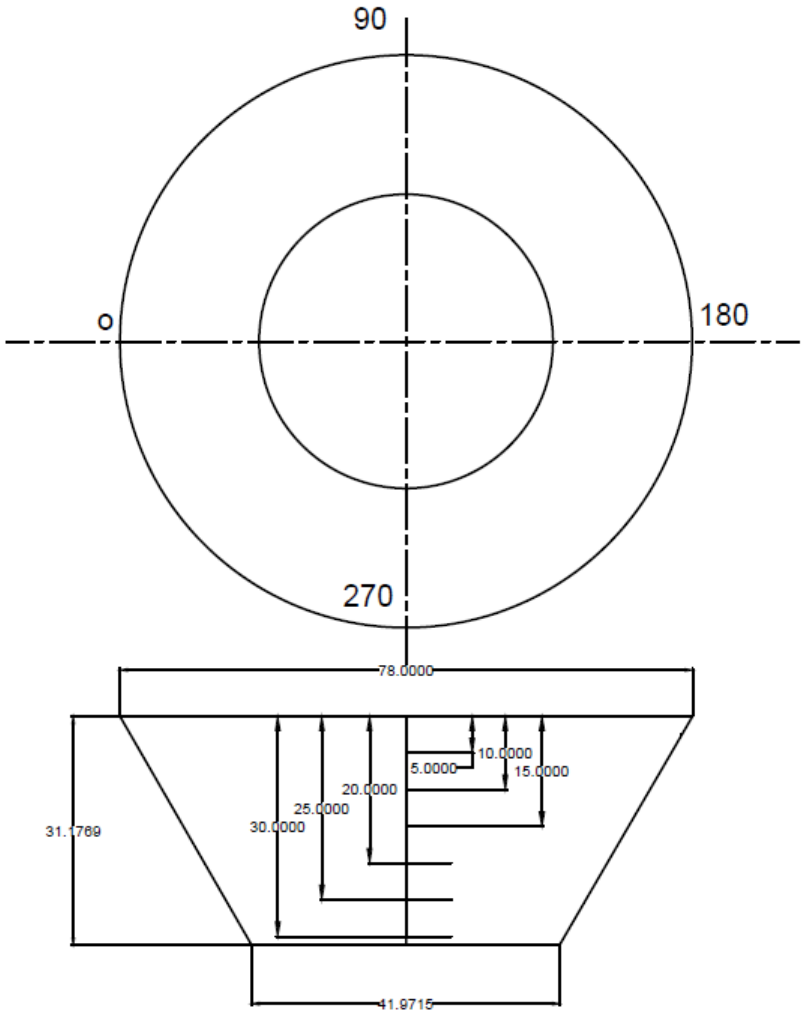

Figure 3.22: Data Location of The Geometry

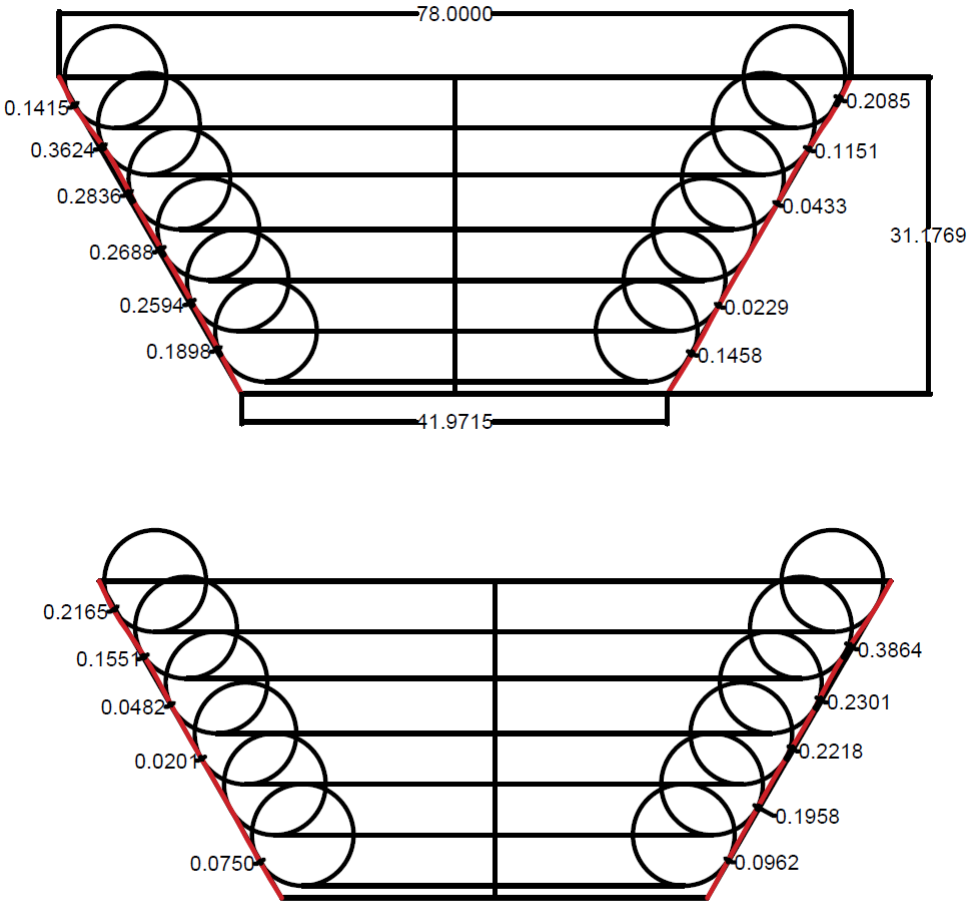

Figure 3.23: Maximum Deviation for RO1

Table 3.8: Geometric Error Measurement data

Sr. No.	Run Order	Deviation at 0	Deviation at 90	Deviation at 180	Deviation at 270
		(mm)	(mm)	(mm)	(mm)
1	1	0.3554	0.2154	0.3401	0.3057
2	2	0.2914	0.3042	0.4897	0.5112
3	3	0.3826	0.3935	0.4212	0.5146
4	4	0.3536	0.3759	0.1924	0.1953
5	5	03780	0.4222	0.1849	0.1592
6	6	0.5419	0.3315	0.3995	0.3242
7	7	0.3624	0.2165	0.2058	0.3864
8	8	0.1647	0.4768	0.3533	0.2280
9	9	0.5150	0.6431	0.4450	0.4696

Table 3.9: Position Data for RO1

0°			90°			180°			270°		
X	Y	Z	X	Y	Z	X	Y	Z	X	Y	Z
mm	mm	mm	mm	mm	mm	mm	mm	mm	mm	mm	mm
-33.423	0	5	0	33.494	5	33.473	0	5	0	-33.247	5
-30.166	0	10	0	30.434	10	30.423	0	10	0	-30.131	10
-27.156	0	15	0	27.425	15	27.373	0	15	0	-27.157	15
-24.282	0	20	0	24.569	20	24.53	0	20	0	-24.268	20
-21.414	0	25	0	21.688	25	21.652	0	25	0	-21.4	25
-18.62	0	30	0	18.921	30	18.897	0	30	0	-18.617	30

Table 3.10: Position Data for RO2

0°			90°			180°			270°		
X	Y	Z	X	Y	Z	X	Y	Z	X	Y	Z
mm	mm	mm	mm	mm	mm	mm	mm	mm	mm	mm	mm
-33.418	0	5	0	33.221	5	33.318	0	5	0	-33.352	5
-30.051	0	10	0	30.013	10	30.3	0	10	0	-30.344	10
-27.07	0	15	0	27.013	15	27.322	0	15	0	-27.288	15
-24.156	0	20	0	24.105	20	24.404	0	20	0	-24.455	20
-21.277	0	25	0	21.244	25	21.5	0	25	0	-21.6	25
-18.44	0	30	0	18.425	30	18.704	0	30	0	-18.691	30

Table 3.11: Position Data for RO3

0°			90°			180°			270°		
X	Y	Z	X	Y	Z	X	Y	Z	X	Y	Z
mm	mm	mm	mm	mm	mm	mm	mm	mm	mm	mm	mm
-33.658	0	5	0	33.491	5	33.162	0	5	0	-33.23	5
-30.533	0	10	0	30.453	10	30.173	0	10	0	-30.205	10
-27.503	0	15	0	27.505	15	27.213	0	15	0	-27.278	15
-24.693	0	20	0	24.658	20	24.343	0	20	0	-24.384	20
-21.829	0	25	0	21.719	25	21.427	0	25	0	-21.453	25
-18.968	0	30	0	18.866	30	18.592	0	30	0	-18.556	30

Table 3.12: Position Data for RO4

0°			90°			180°			270°		
X	Y	Z	X	Y	Z	X	Y	Z	X	Y	Z
mm	mm	mm	mm	mm	mm	mm	mm	mm	mm	mm	mm
-33.371	0	5	0	33.137	5	33.245	0	5	0	-33.355	5
-29.93	0	10	0	29.863	10	30.14	0	10	0	-30.124	10
-26.916	0	15	0	26.843	15	27.124	0	15	0	-27.166	15
-24.015	0	20	0	23.917	20	24.187	0	20	0	-24.228	20
-21.091	0	25	0	21.063	25	21.308	0	25	0	-21.339	25
-18.279	0	30	0	18.255	30	18.528	0	30	0	-18.522	30

Table 3.13: Position Data for RO5

0°			90°			180°			270°		
X	Y	Z	X	Y	Z	X	Y	Z	X	Y	Z
mm	mm	mm	mm	mm	mm	mm	mm	mm	mm	mm	mm
-33.458	0	5	0	33.313	5	33.45	0	5	0	-33.448	5
-30.22	0	10	0	30.177	10	30.486	0	10	0	-30.638	10
-27.239	0	15	0	27.219	15	27.513	0	15	0	-27.499	15
-24.399	0	20	0	24.381	20	24.624	0	20	0	-24.622	20
-21.493	0	25	0	21.553	25	21.739	0	25	0	-21.805	25
-18.63	0	30	0	18.631	30	18.898	0	30	0	-18.903	30

Table 3.14: Position Data for RO6

0°			90°			180°			270°		
X	Y	Z	X	Y	Z	X	Y	Z	X	Y	Z
mm	mm	mm	mm	mm	mm	mm	mm	mm	mm	mm	mm
-33.607	0	5	0	33.959	5	33.372	0	5	0	-33.367	5
-30.207	0	10	0	30.249	10	30.11	0	10	0	-29.963	10
-27.231	0	15	0	27.308	15	27.141	0	15	0	-27.007	15
-24.303	0	20	0	24.406	20	24.251	0	20	0	-24.095	20
-21.53	0	25	0	21.488	25	21.198	0	25	0	-21.224	25
-18.721	0	30	0	18.65	30	18.368	0	30	0	-18.401	30

Table 3.15: Position Data for RO7

0°			90°			180°			270°		
X	Y	Z	X	Y	Z	X	Y	Z	X	Y	Z
mm	mm	mm	mm	mm	mm	mm	mm	mm	mm	mm	mm
-33.59	0	5	0	33.338	5	33.069	0	5	0	-33.067	5
-30.397	0	10	0	30.257	10	30.002	0	10	0	-29.979	10
-27.447	0	15	0	27.209	15	27.01	0	15	0	-27.013	15
-24.541	0	20	0	24.311	20	24.079	0	20	0	-24.125	20
-21.613	0	25	0	21.456	25	21.214	0	25	0	-21.242	25
-18.789	0	30	0	18.647	30	18.406	0	30	0	-18.4	30

Table 3.16: Position Data for RO8

0			90			180			270		
X	Y	Z	X	Y	Z	X	Y	Z	X	Y	Z
mm	mm	mm	mm	mm	mm	mm	mm	mm	mm	mm	mm
-33.59	0	5	0	33.244	5	33.185	0	5	0	-33.367	5
-30.31	0	10	0	30.029	10	30.073	0	10	0	-30.248	10
-27.337	0	15	0	26.991	15	27.019	0	15	0	-27.211	15
-24.408	0	20	0	24.042	20	24.116	0	20	0	-24.261	20
-21.523	0	25	0	21.186	25	21.264	0	25	0	-21.435	25
-18.697	0	30	0	18.448	30	18.552	0	30	0	-18.726	30

Table 3.17: Position Data for RO9

0°			90°			180°			270°		
X	Y	Z	X	Y	Z	X	Y	Z	X	Y	Z
mm	mm	mm	mm	mm	mm	mm	mm	mm	mm	mm	mm
-33.318	0	5	0	33.152	5	33.212	0	5	0	-33.187	5
-29.91	0	10	0	29.899	10	30.091	0	10	0	-30.12	10
-27.1	0	15	0	26.852	15	27.039	0	15	0	-26.977	15
-24.014	0	20	0	23.88	20	24.079	0	20	0	-24.014	20
-21.091	0	25	0	20.945	25	21.207	0	25	0	-21.341	25
-18.377	0	30	0	18.305	30	18.552	0	30	0	-18.584	30

Table 3.18: Position Data for r = 3 mm, sd = 0.50 mm

0°			90°			180°			270°		
X	Y	Z	X	Y	Z	X	Y	Z	X	Y	Z
mm	mm	mm	mm	mm	mm	mm	mm	mm	mm	mm	mm
-33.282	0	5	0	33.301	5	33.148	0	5	0	-33.066	5
-30.218	0	10	0	30.232	10	30.11	0	10	0	-30.094	10
-27.354	0	15	0	27.313	15	27.165	0	15	0	-27.157	15
-24.433	0	20	0	24.391	20	24.272	0	20	0	-24.235	20
-21.55	0	25	0	21.453	25	21.407	0	25	0	-21.474	25
-18.778	0	30	0	18.602	30	18.524	0	30	0	-18.521	30

Table 3.19: Position Data for r = 7 mm, sd= 0.50 mm

0°			90°			180°			270°		
X	Y	Z	X	Y	Z	X	Y	Z	X	Y	Z
mm	mm	mm	mm	mm	mm	mm	mm	mm	mm	mm	mm
-33.334	0	5	0	33.416	5	33.558	0	5	0	-33.308	5
-30.195	0	10	0	30.125	10	30.263	0	10	0	-30.21	10
-27.318	0	15	0	27.197	15	27.286	0	15	0	-27.328	15
-24.311	0	20	0	24.158	20	24.336	0	20	0	-24.351	20
-21.43	0	25	0	21.421	25	21.444	0	25	0	-21.508	25
-18.604	0	30	0	18.545	30	18.652	0	30	0	-18.65	30

Chapter 4

FEA Simulation using LS-DYNA Software

4.1 FEA simulation of preliminary experiment

The simulation of Single point incremental forming for cone test is performed using LSDYNA software. Pre-processing and Post-processing is carried out in LS-PrePost 4.1.

4.1.1 Idealized FEA model

The CAD model was generated in LS-DYNA Pre-post. Tool is idealized as sphere of radius 4 mm, 5 mm and 6 mm. Tool and blank are meshed by BT-Shell elements. Also, backing plates are modeled with 2 mm radius. Initially distance between tool and blank is maintained as 10 mm. In Fig. 4.1 relative position of tool (1), sheet (2), and backing plate (3) are shown. The contact between tool to sheet and sheet to backing plate is given by FORMING_ONE_ WAY_SURFACE_TO_SURFACE keyword. the value of static friction is 0.125 and dynamic friction is 0.395. Using Time vs Position data for the motion of the tool is generated using DEFINE_CURVE keyword. Motion of the tool is assigned using BOUNDARY_ PRESCRIBED_ MOTION_RIGID keyword.

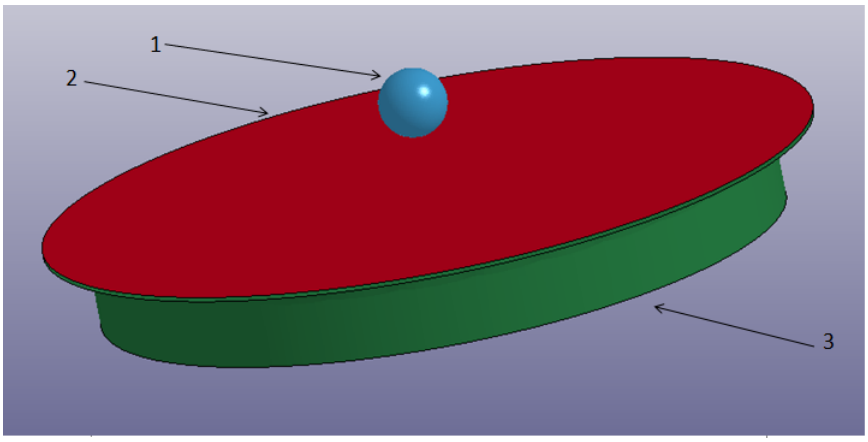

Figure 4.1: Idealized FEA model

Table 4.1: Keywords for simulation

Sr. No			Keywords
1	Material	For sheet	MAT_18_POWER_LAW_PLASTICITY
		For tool	MAT_20_RIGID
2	Boundary	For sheet	BOUNDARY_SPC_SET
		For tool	BOUNDARY_PRESCRIBED_MOTION_RIGID
3	Contacts		FORMING_ONE_WAY_SURFACE_TO_SURFACE
4	Tool Motion		DEFINE_CURVE

4.1.2 Material property

Material property for tool and sheet are as per Table 3.15. For tool E =2.000e+005 N/mm2 and Poisson ratio = 0.30 which is considered as a rigid material model.

Table 4.2: Material properties for sheet and tool

For Sheet	Mass density	2.710e-006
	Young Modulus	5.579e+004 N/mm2
	Poisson Ratio	0.3300000
	Strength Co-efficient	209.28670
	Hardening Exponent	0.5376000
	Initial yield stress	111.0000
For Tool	Mass density	7.850e-006
	Young Modulus	2.000e+005 N/mm2
	Poisson Ratio	0.3000000
Tool to sheet contact	Static Friction	0.125
	Dynamic Friction	0.395
Backing Plate to Sheet Contact	Static Friction	0.125
	Dynamic Friction	0.395

4.2 Simulation Result of Preliminary Experiment

After Performing simulation to measure the actual depth of the formed component, component is cut from the center by a plain perpendicular to z axis as shown in fig 4.2.

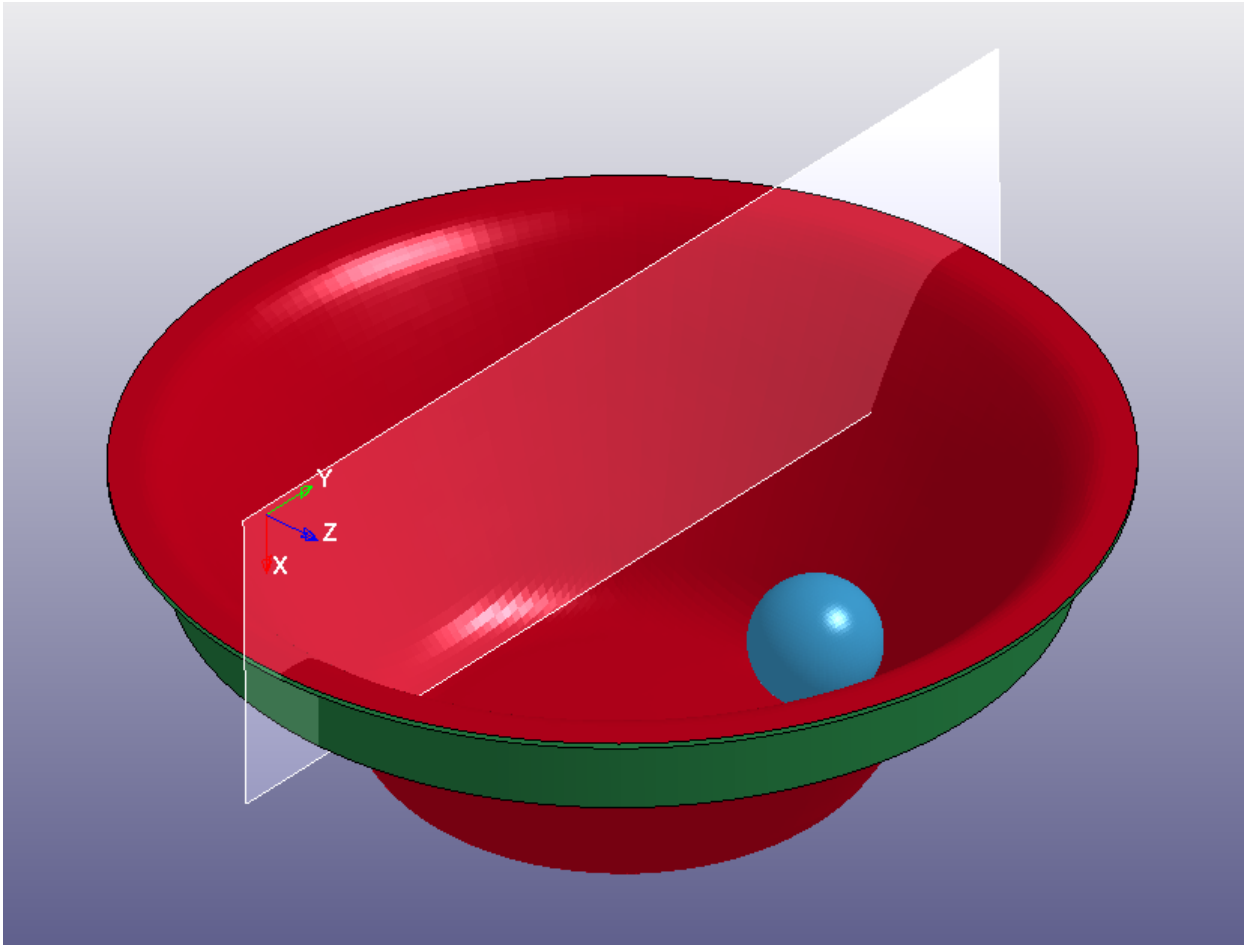

Figure 4.2: Measurement of height

Figure 4.3 Shows the cut section of RO1. In the RO1 radius is 4 mm and step depth is 0.25 mm. theoretical height of this component is 31.1769 mm but due to spring back actual height comes out to be 30.085 mm Figure 4.4 to 4.11 shows the cut sections of RO2 to RO9

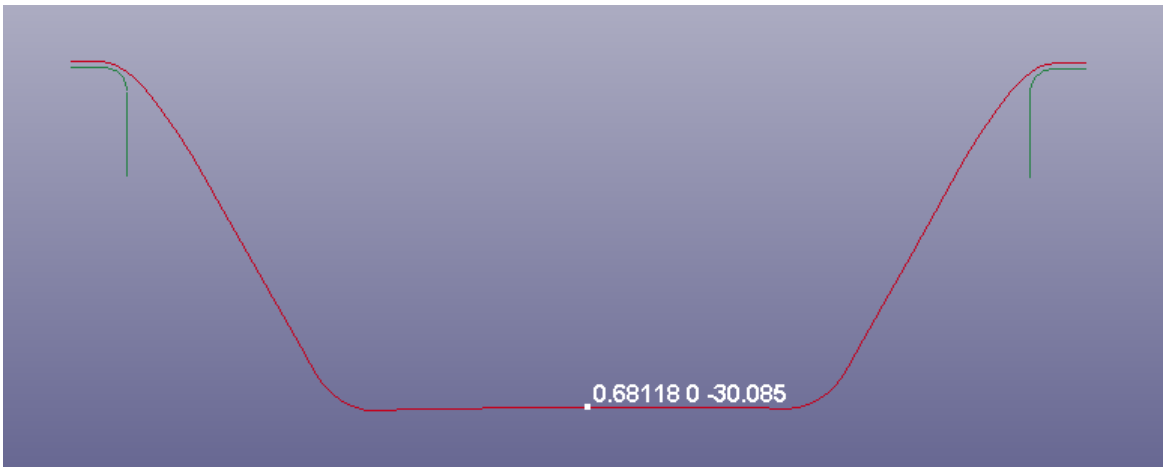

Figure 4.3: Cut section of Run Order 1 (r = 6 mm, sd = 0.25 mm)

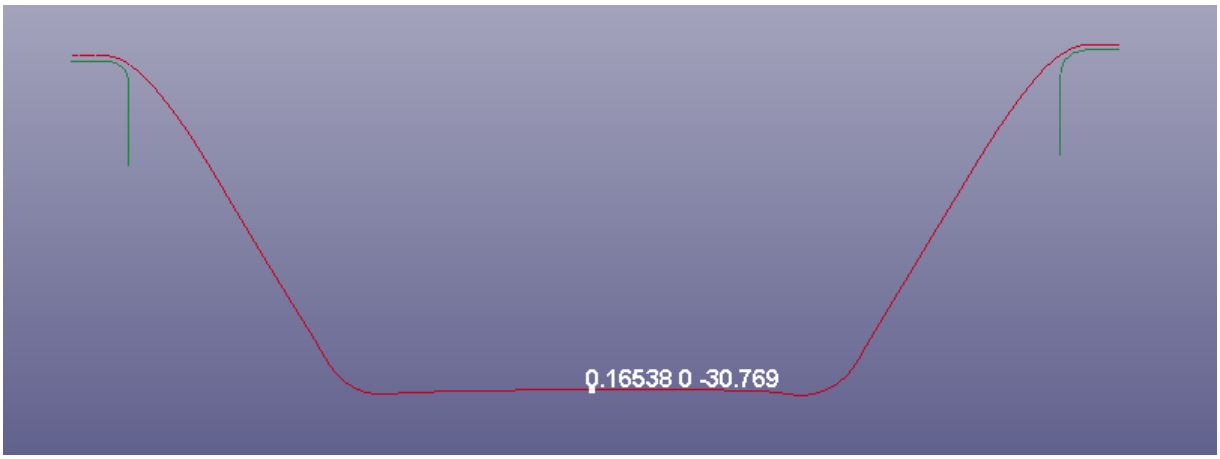

Figure 4.4: Cut section of Run Order 2 (r = 5 mm, sd = 0.50 mm)

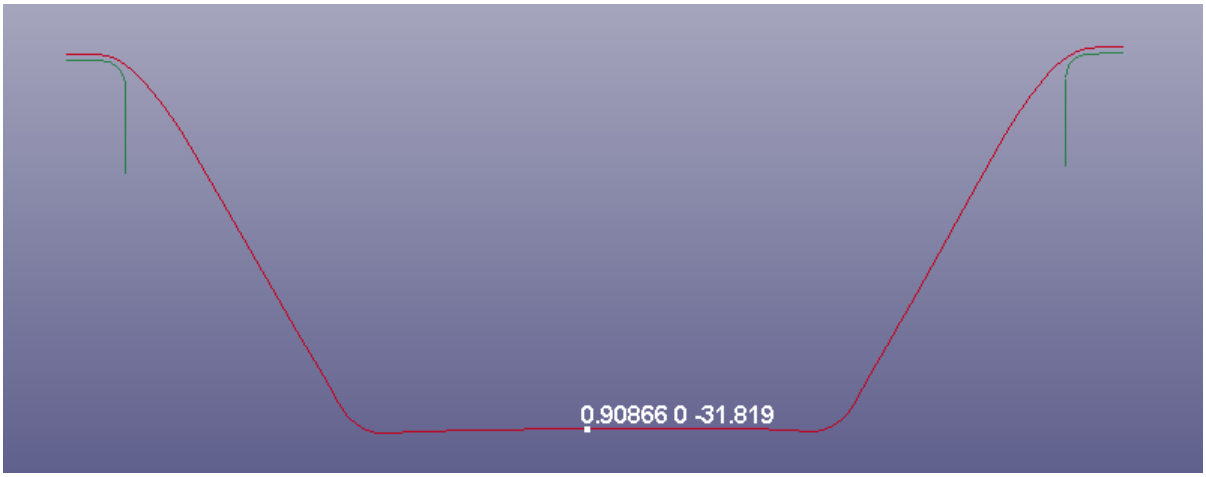

Figure 4.5: Cut section of Run Order 3 (r = 4 mm, sd = 0.25 mm)

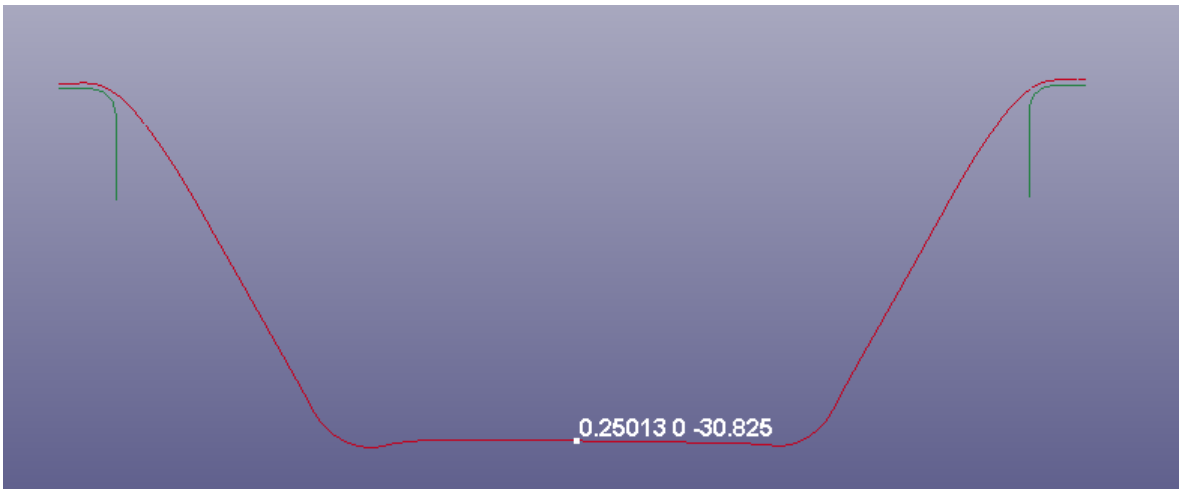

Figure 4.6: Cut section of Run Order 4 (r = 5 mm, sd = 0.75 mm)

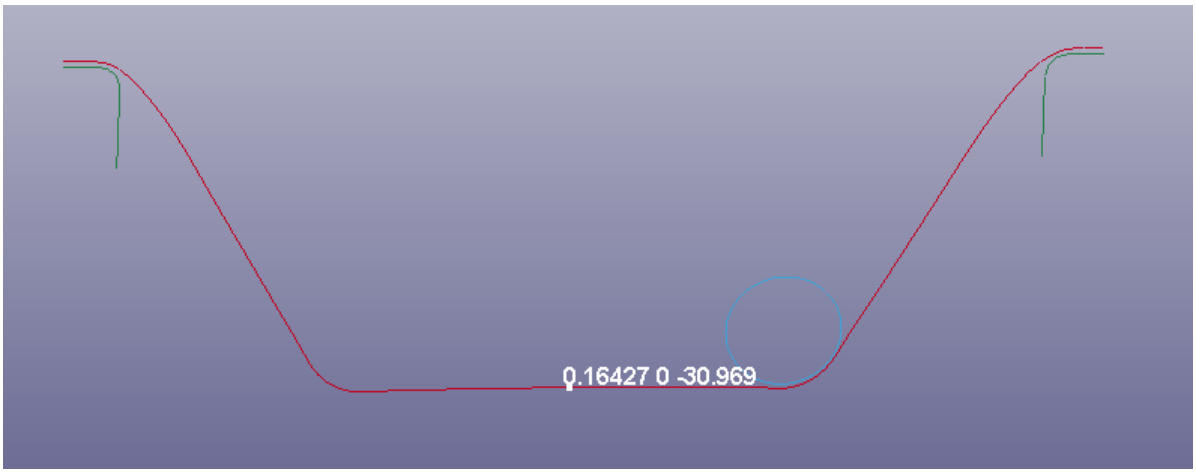

Figure 4.7: Cut section of Run Order 5 (r = 5 mm, sd = 0.25 mm)

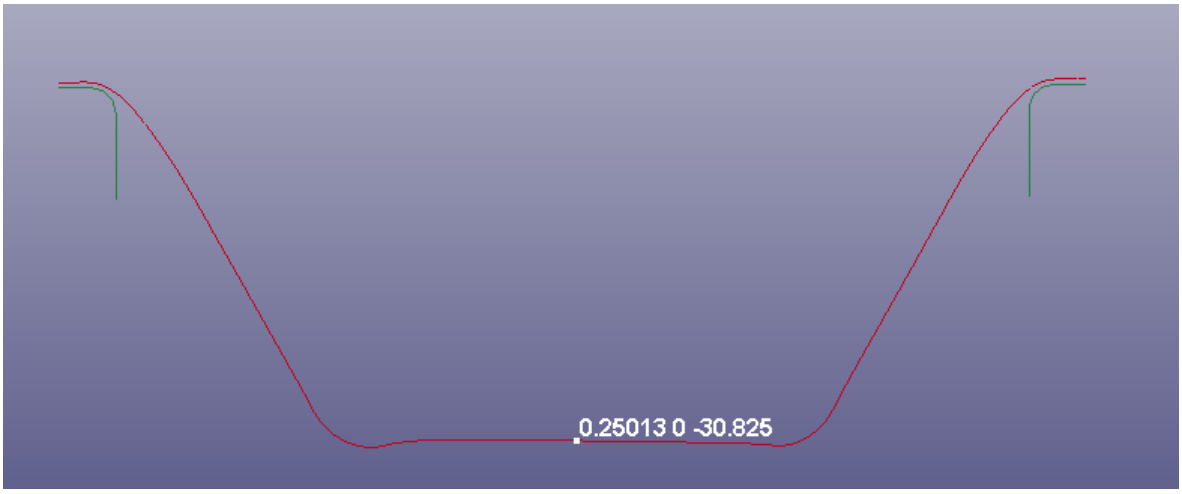

Figure 4.8: Cut section of Run Order 6 (r = 4 mm, sd = 0.75 mm)

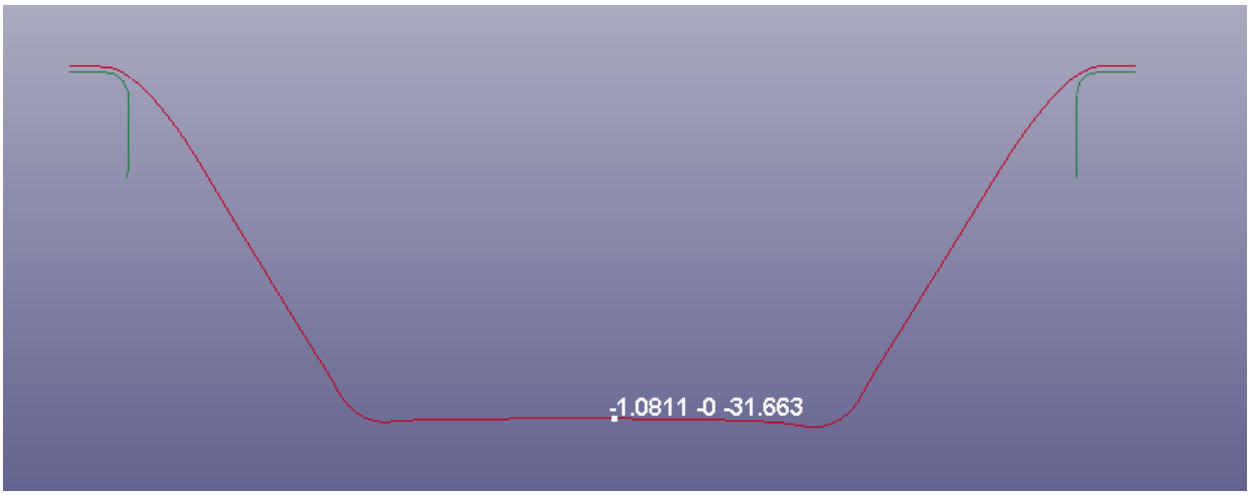

Figure 4.9: Cut section of Run Order 7 (r = 4 mm, sd = 0.50 mm)

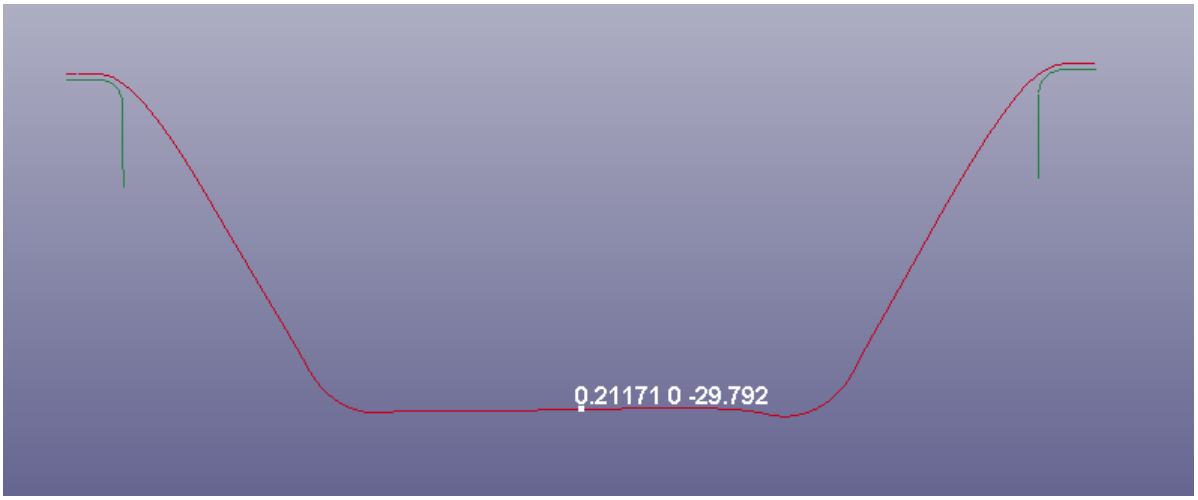

Figure 4.10: Cut section of Run Order 8 (r = 6 mm, sd = 0.50 mm)

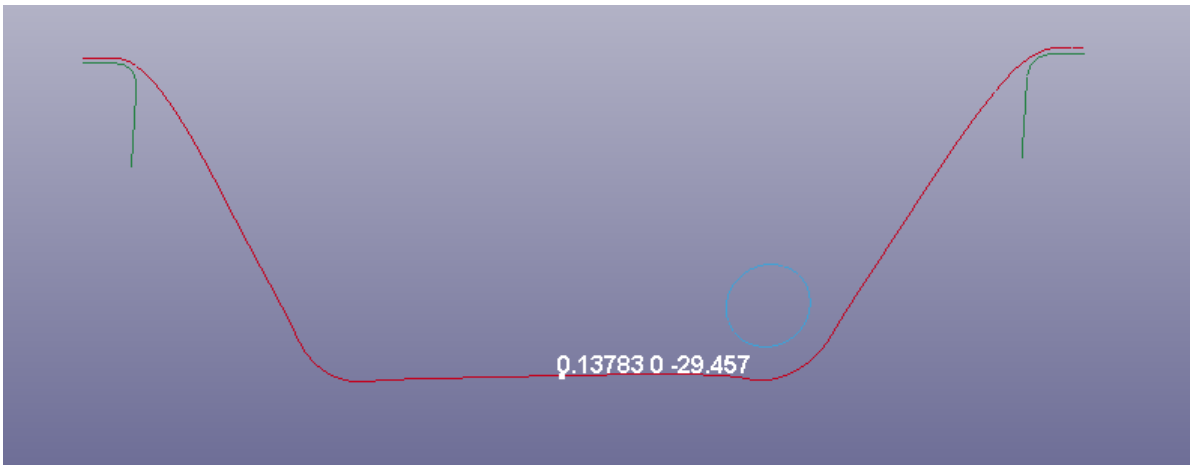

Figure 4.11: Cut section of Run Order 9 (r = 6 mm, sd = 0.75 mm)

Chapter 5

Results and Discussion

5.1 Result of Experiment and Simulation

Summary of Actual depth and depth obtained by simulation is summarized in table 5.1.Table also shows measured and simulated pillow depth. Table 5.2 gives the difference between experimental and simulation depth for each Runorder. Maximum difference of the order is 4.3 %. Figure 5.1 gives the main effects plot for pillow depth. Figure 5.2 gives interaction plot for pillow depth. Main effects plot suggests that as tool radius increases pillow depth decreases. Also as step depth increases pillow depth increases. No significant interaction is found between tool radius and step depth on pillow defect. Figure 5.3 shows pillow depth for different tool radius. Here additional experiments are performed at tool radius 3, 5 and 7 mm. It also shows clear trend of the reduced pillow depth with increase in tool radius. Fig 5.4 shows main effects plot for geometric error. As tool radius and step depth increases, geometric error increases.

Table 5.1: Pillow Defect Result after Simulation

RunOrder	Tool Radius (mm)	Step Depth (mm)	Original Depth (mm)	Actual Depth (mm)	Depth by Simulation (mm)	Pillow depth of Experiment (mm)	Pillow depth of Simulation (mm)
1	6	0.25	31.1769	30.847	30.103	0.3299	1.0745
2	5	0.5	31.1769	31.144	30.798	0.0329	0.3781
3	4	0.25	31.1769	30.717	31.824	0.4599	0.6477
4	5	0.75	31.1769	31.086	30.958	0.0909	0.2173
5	5	0.25	31.1769	30.816	30.969	0.3608	0.2079
6	4	0.75	31.1769	30.364	31.565	0.8129	0.3885
7	4	0.5	31.1769	30.637	31.672	0.5399	0.4978
8	6	0.5	31.1769	30.895	29.792	0.2819	1.3849
9	6	0.75	31.1769	30.785	29.461	0.3919	1.7146

Table 5.2: Difference of Experiment and Simulation

RunOrder	Tool Radius	Step Depth	Actual Depth	Depth after Simulation	Difference
	(mm)	(mm)	(mm)	(mm)	(%)
1	6	0.25	30.847	30.103	2.41
2	5	0.5	31.144	30.798	1.10
3	4	0.25	30.717	31.824	3.60
4	5	0.75	31.086	30.958	0.40
5	5	0.25	30.816	30.969	0.49
6	4	0.75	30.364	31.565	3.95
7	4	0.5	30.637	31.672	3.37
8	6	0.5	30.895	29.792	3.57
9	6	0.75	30.785	29.461	4.3

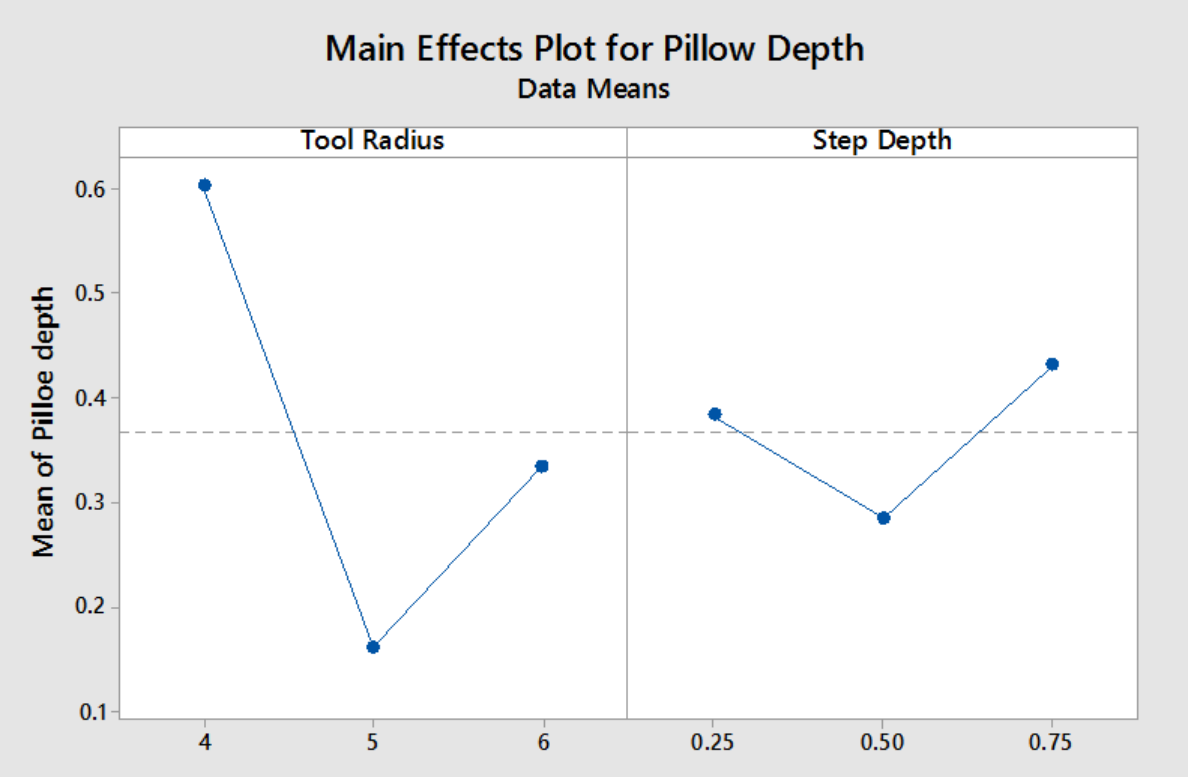

Figure 5.1: Main effect plots for pillow depth

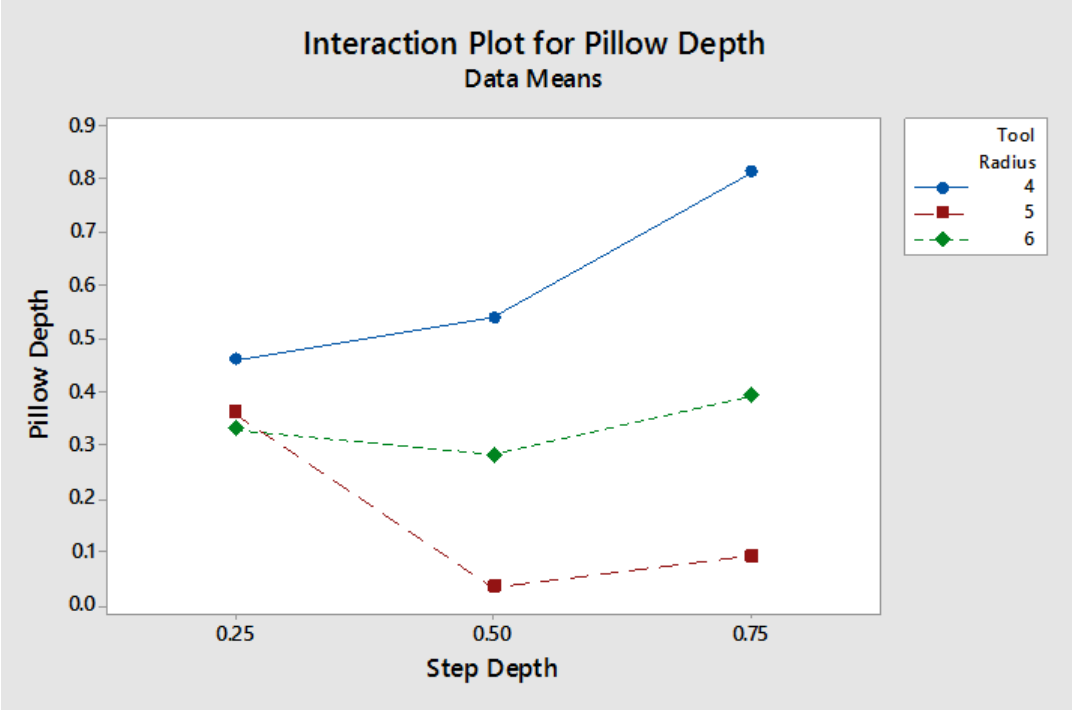

Figure 5.2: Interaction plot for Pillow Depth

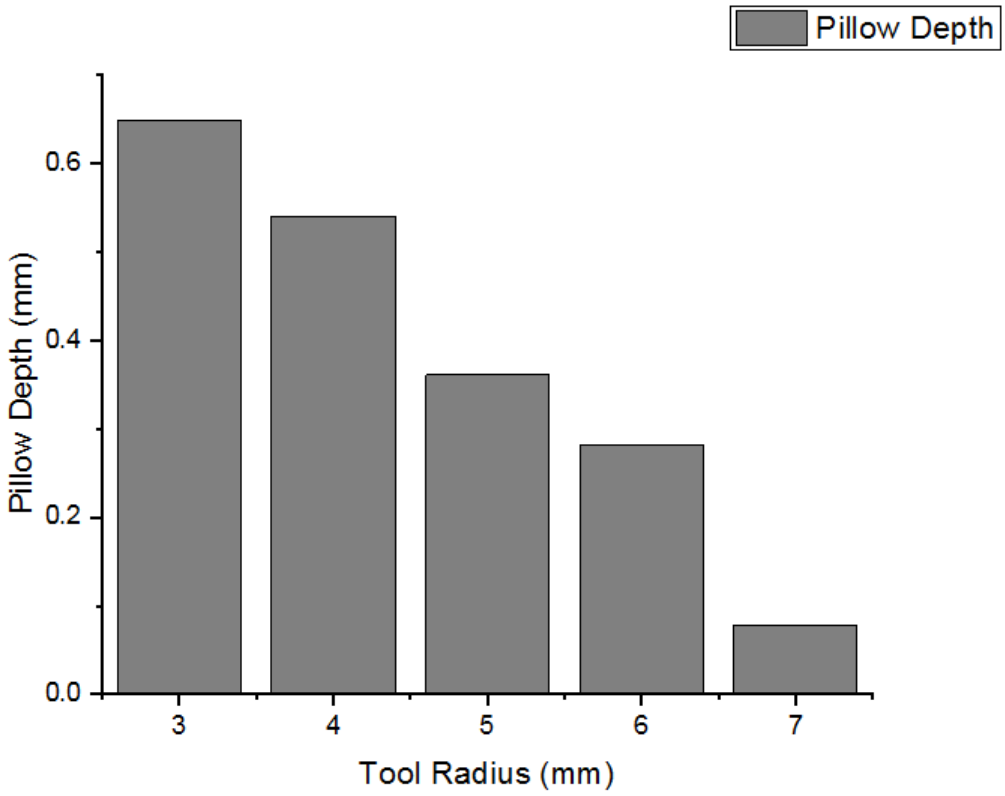

Figure 5.3: Pillow Depth at Different tool radius

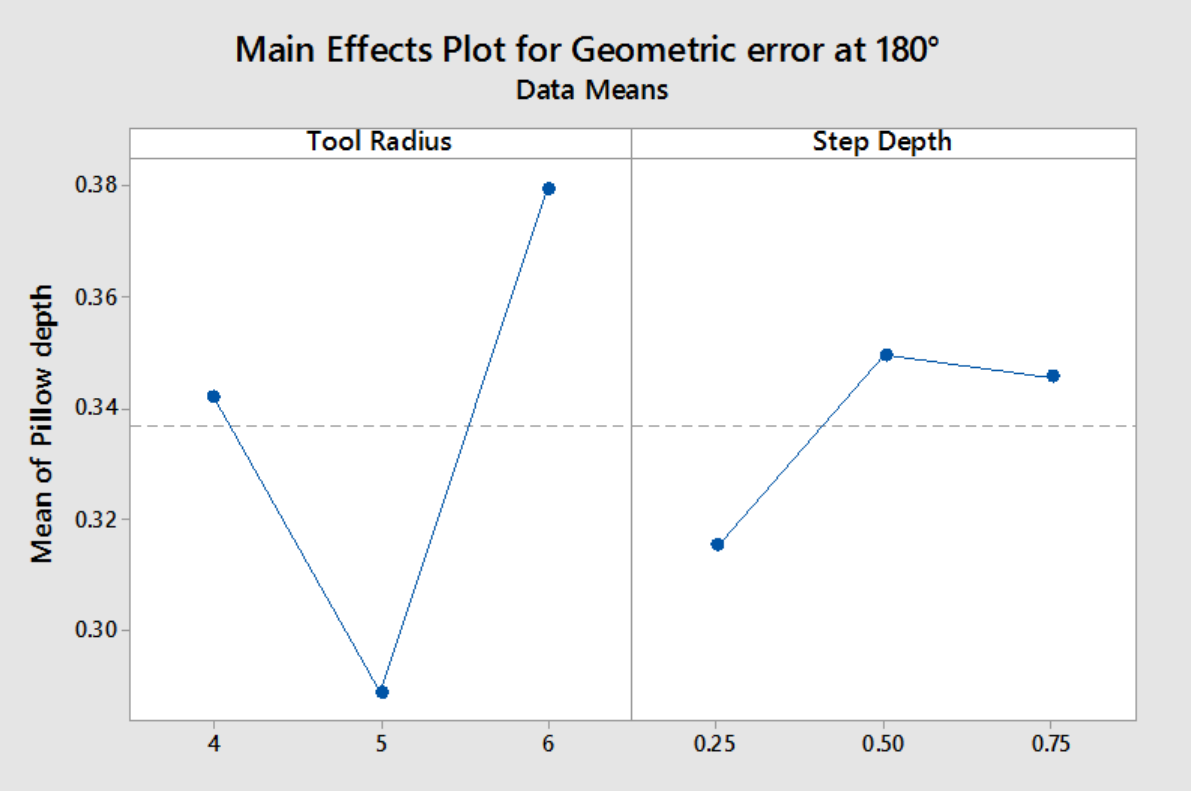

Figure 5.4: Main Effects plot for Geometric Error

Chapter 6

Conclusion and Future scope

Conclusion:

Annealing Process results shows that heating temperature of 343℃ and heating time of 10 min is most suitable to obtain 6 micron grain size.

As size of the tool increases pillow depth decreases as step depth increases pillow depth increases. This is because of reason the with large step depth at the corner center of the sheet moves up by larger amount. Also as size of the tool increases results in to poor geometric accuracy.

Future scope:

Measurement of pillow depth for other shapes.

References

[1] L-W Ma and J-H MGabriel Centeno , Isabel Bagudanch, A. J. Martinez- Donaire, M. L. Gracia-Romeu, C.Valleano"Asymmetric single point incremental forming of sheet metal." CIRP Annals-Manufacturing Technology 54.2 (2005): 88-114.

[2] León, J. "Analysis of the influence of geometrical parameters on the mechanical properties of incremental sheet forming parts." Procedia Engineering 63 (2013): 445-453.

[3] L-W Ma and J-H MGabriel Centeno , Isabel Bagudanch, A. J. Martinez- Donaire, M. L. Gracia-Romeu, C.Valleano. "Critical analysis of necking and fracture limit strains and forming forces in single-point incremental forming." Materials & Design63 (2014): 20-29.

[4] Hussain, G., and L. Gao. "A novel method to test the thinning limits of sheet metals in negative incremental forming." International Journal of Machine Tools and Manufacture 47.3 (2007): 419-435.

[5] Al-Ghamdi, K. A., G. Hussain, and Shahid I. Butt. "Force variations with defects and a force-based strategy to control defects in SPIF." Materials and Manufacturing Processes 29.10 (2014): 1197-1204.

[6] Singh, Arshpreet, and Anupam Agrawal. "Comparison of deforming forces, residual stresses and geometrical accuracy of deformation machining with conventional bending and forming." Journal of Materials Processing Technology 234 (2016): 259-271.

[7] Hussain, H. R. Khan , L. Gao & N. Hayat . "Guidelines for tool-size selection for single-point incremental forming of an aerospace alloy." Materials and Manufacturing Processes 28.3 (2013): 324-329.

[8] Petek, Aleš, Karl Kuzman, and Blaž Suhač. "Autonomous on-line system for fracture identification at incremental sheet forming." CIRP Annals-Manufacturing Technology 58.1 (2009): 283-286

[9] Suresh, Kurra, and Srinivasa Prakash Regalla. "Analysis of formability in single point incremental forming using finite element simulations." Procedia Materials Science 6 (2014): 430-435.

[10] J. Leona, D. Salcedo, C. Ciaurriza, C.J. Luis, J.P. Fuertes, I. Puertas, R. Luri. "Analysis of the influence of geometrical parameters on the mechanical properties of incremental sheet forming parts." Procedia Engineering 63 (2013): 445-453.

[11] L. Fratini , G. Ambrogio , R. Di Lorenzo , L. Filice, F. Micari . "Influence of mechanical properties of the sheet material on formability in single point incremental forming." CIRP Annals-Manufacturing Technology 53.1 (2004): 207-210.

[12] E Hagan, and J. Jeswiet. "Analysis of surface roughness for parts formed by computer numerical controlled incremental forming." Proceedings of the Institution of Mechanical Engineers, Part B: Journal of Engineering Manufacture 218.10 (2004): 1307-1312.

[13] Joost Du ou , Yasemin Tunckol , Alex Szekeres, Paul Vanherck . "Experimental study on force measurements for single point incremental forming." Journal of Materials Processing Technology 189.1 (2007): 65-72.

[14] W.C. Emmensa , A.H. van den Boogaard "An overview of stabilizing deformation mechanisms in incremental sheet forming." Journal of Materials Processing Technology 209.8 (2009): 3688-3695.

[15] Vahdati, Mehdi, Ramezanali Mahdavinejad, and Saeid Amini. "Investigation of the ultrasonic vibration effect in incremental sheet metal forming process." Proceedings of the Institution of Mechanical Engineers, Part B: Journal of Engineering Manufacture (2015): 0954405415578579.

[16] Z. Jeswiet, J. "Asymmetric single point incremental forming of sheet metal." CIRP Annals-Manufacturing Technology 54.2 (2005): 88-114.

[17] I. Bagudancha , M.L. Garcia-Romeua, I. Ferrera, J. Lupia˜nez. "The effect of process parameters on the energy consumption in Single Point Incremental Forming." Procedia Engineering 63 (2013): 346-353.

[18] Guzmán, Carlos Felipe. "Study of the geometrical inaccuracy on a SPIF two-slope pyramid by finite element simulations." International Journal of Solids and Structures 49.25 (2012): 3594-3604.

[19] Allwood, Julian M., Daniel Braun, and Omer Music. "The effect of partially cut-out blanks on geometric accuracy in incremental sheet forming." Journal of Materials Processing Technology 210.11 (2010): 1501-1510.

[20] Al-Ghamdi, K. A., and G. Hussain. "The pillowing tendency of materials in single-point incremental forming: experimental and finite element analyses." Proceedings of the Institution of Mechanical Engineers, Part B: Journal of Engineering Manufacture 229.5 (2015): 744-753.

[21] Bagudanch, I.. "Forming force and temperature effects on single point incremental forming of polyvinylchloride." Journal of materials processing technology 219 (2015): 221-229.

[22] Ma, L. W., and J. H. Mo. "Three-dimensional finite element method simulation of sheet metal single-point incremental forming and the deformation pattern analysis." Proceedings of the Institution of Mechanical Engineers, Part B: Journal of Engineering Manufacture 222.3 (2008): 373-38

[23] Radu, Crina, et al. "The effect of residual stresses on the accuracy of parts processed by SPIF." Materials and Manufacturing Processes 28.5 (2013): 572-576

[24] Young, D., and J. Jeswiet. "Wall thicknes in single point incremental forming ." Proceedings of the institution of Mechanical Engineers, Part B: Journal of Engineering Manufacture, 218.11 (2004): 1453-1459

[25] Aniket Patel. "Effect of process parameters on forming forces in Single Point Incremental Forming (SPIF) process"